Geophys. J. R. astr. Soc. (1970) **20,** 509–542.

The Implications of Terrestrial Heat Flow Observations on Current Tectonic and Geochemical Models of the Crust and Upper Mantle of the Earth

John G. Sclater and Jean Francheteau

(Received 1970 January 28)

Summary

The average heat flow through continental orogenic belts decreases with the age of the orogeny to an approximately constant value for the Precambrian shields and platforms. The average heat flow for provinces of the North Pacific decreases with the age of the province. The mean heat flow through the province younger than 10 million years is 2·82 μ cal $cm^{-2}\,s^{-1}$ whereas the mean heat flow through provinces older than the middle Cretaceous is 1·15μ cal $cm^{-2}\,s^{-1}$. The contrast in the chemical composition of continental and oceanic crustal rocks and the disparity in time scale for the decay of heat flow suggest a different explanation for the heat flow through oceans and continents. The observed equality of the mean oceanic and continental heat flows may not be relevant to evaluating the thermal contribution of the upper mantle.

Two geophysical and geochemical models of the oceanic and continental crust and upper mantle are presented. Both can explain the near equality of heat flow through the Precambrian shields and the old ocean basins when plates of continental and oceanic lithosphere are allowed to move. The oceanic lithosphere is approximately 100 km thick and the mantle is assumed to be the same under both the continents and oceans. The models differ principally in the condition assigned to their lower boundary. These conditions result in two different geochemical compositions for the oceanic lithosphere. Both oceanic models can explain the flow of heat through the North Pacific and the topography of the East Pacific Rise. If the effects of water in the mantle and subsolidus phase changes are considered, the lithosphere could be as thin as 75 km and still consistent with the heat flow and topographic anomalies.

The models also account for the elevation of the mid-Atlantic ridge and the gross structure of the heat flow through the South Atlantic. The loss of heat in creating oceanic lithosphere may be as much as 45 per cent of the total average heat flow of the Earth. Heat lost by this process can no longer be ignored in models of the thermal history of the Earth.

1. Introduction

Since the first reliable determinations of heat flow in England (Benfield 1939; Anderson 1939) and in South Africa (Bullard 1939), the number of observation points has grown considerably in the last decade, chiefly due to measurements made at sea. Lee & Uyeda (1965), on the basis of 131 continental and 913 oceanic measure-

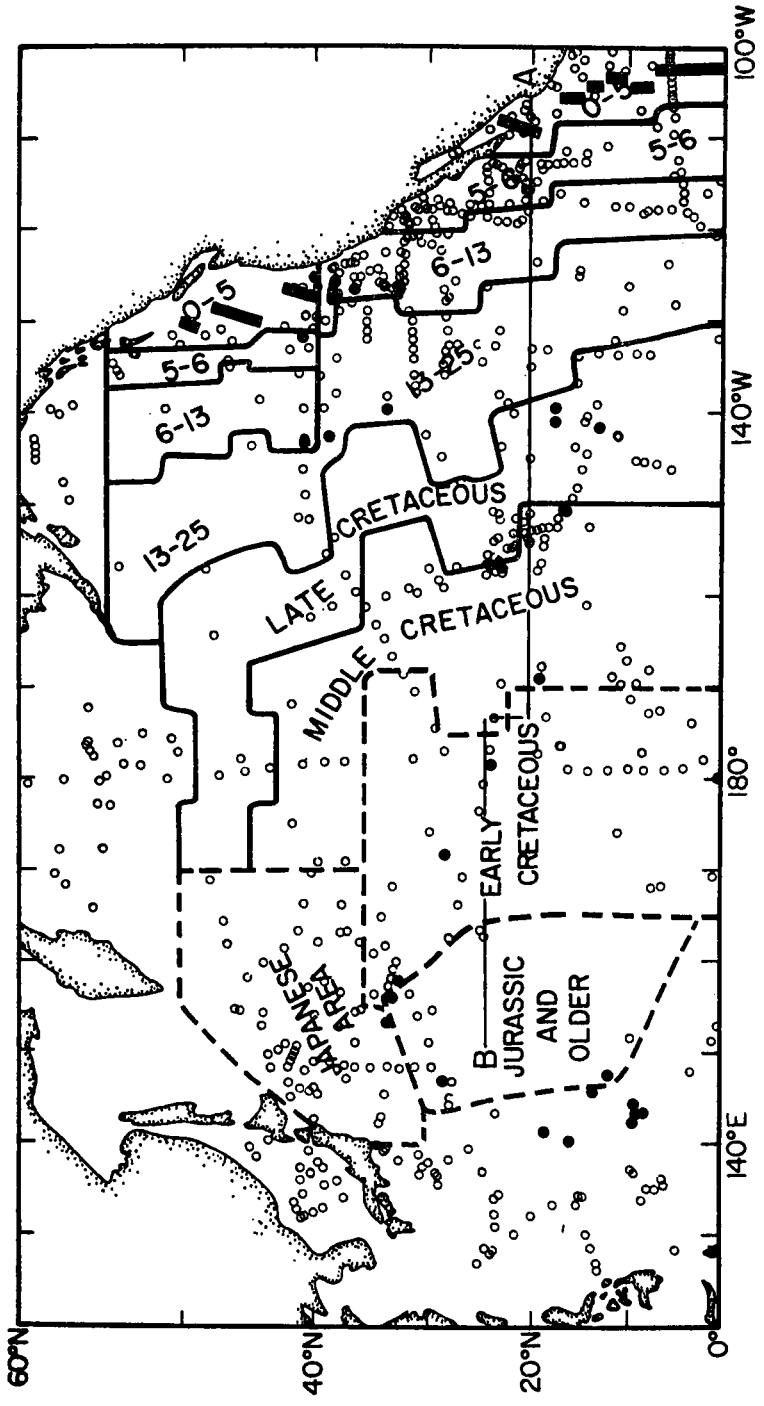

FIG. 1. Provinces of the North Pacific. The boundaries of the provinces are determined from magnetic lineations (Atwater & Menard 1970) and the age of sediment recovered by JOIDES deep sea drillings (McManus & Burns 1969; Scientiff Staff, Leg VI, 1969). The thick black line is the crest of the East Pacific Rise, Gorda and Juan de Fuca ridges. The open circles are the locations of the heat flow measurements and the filled-in circles are the locations of the JOIDES deep sea drillings. AB is the location of the topographic profile of Udintsev (1964).

ments, proposed the following arithmetic means for continental, oceanic and planetary heat flows—1·43, 1·60, and 1·58 μ cal cm^{-2} s^{-1} respectively. It is likely that the difference between the oceanic and continental means is not significant and is largely a consequence of over representation of the mid-ocean ridges which have high values and of the omission of volcanic areas on land. When the observations are averaged over five-degree squares, the means of the continental and oceanic squares are 1·49 and 1·47 μ cal cm^{-2} s^{-1} respectively (Lee & Uyeda 1965).

It is usually supposed that most of the heat arriving at the surface is produced by radioactivity within the Earth. Because of the difference in radioactive content of the oceanic and continental crustal rocks, it was generally expected that the heat flow at sea would be less than that on land. The discovery that the two are equal poses a difficult problem (Bullard 1952; Bullard 1968).

In this paper, we attempt to answer this problem by analysing in more detail the distribution of heat flow values both on land and on the ocean floor. The explanation offered for the differing distribution of heat through continents and oceans reconciles terrestrial heat flow observations and plate tectonics and has strong implications for geochemical and thermal models of the Earth.

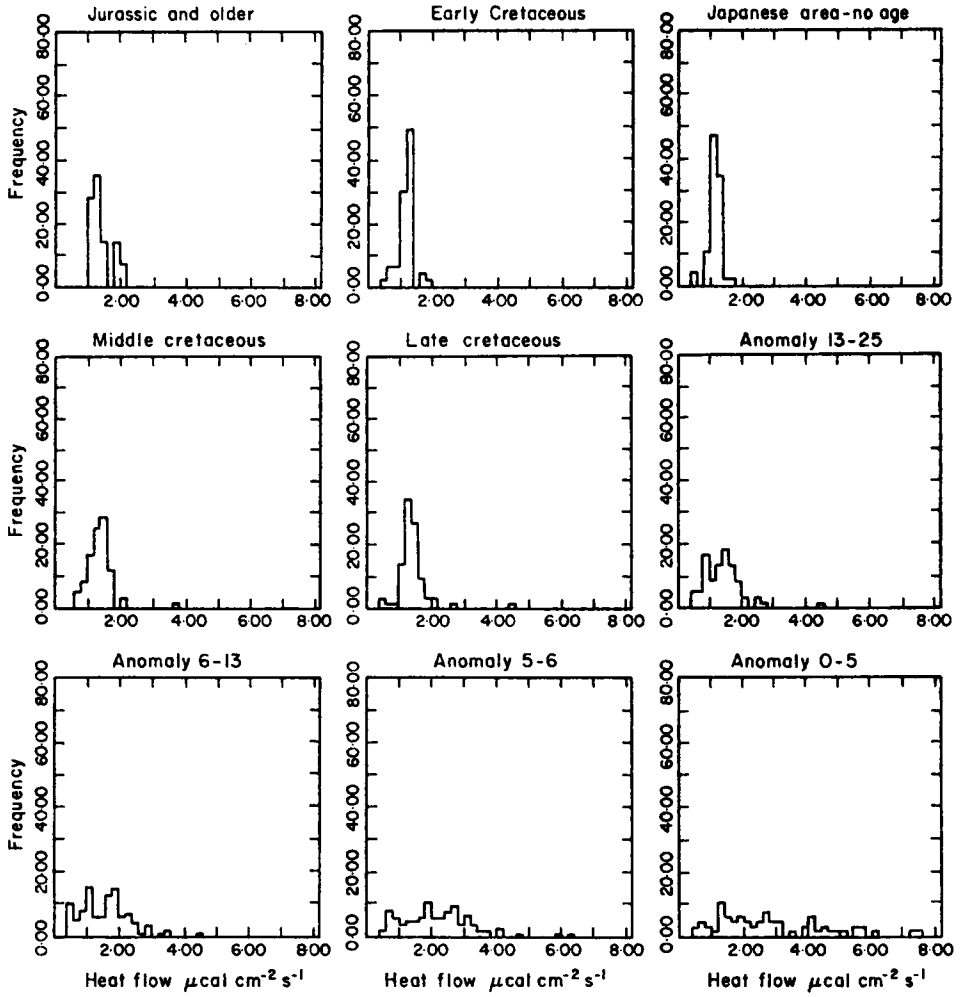

FIG. 2. Histograms of the distribution of heat flow values in the nine North Pacific provinces.

2. Heat flow in the North Pacific

In the sea-floor spreading model, new crust is created by the intrusion of hot material along the centre of spreading. The new material cools and solidifies and moves away from the centre of spreading while more crust is intruded. McKenzie (1967) and Langseth & Von Herzen (in press) have shown that such a model is compatible with observed heat flow data. It explains the broad band of high values near the crest of the mid-ocean ridges and the general decrease of heat flow with increasing distance from the ridge crest. However, the plots of heat flow versus distance from the crest of ridges as shown by Lee & Uyeda (1965) are not suitable for detailed comparison with the theoretical models. These plots take no account of (a) the offsets of the ridge axis by transform faults, (b) the changes in velocity of spreading, and (c) the increased scatter in the measurement, as the crest of the ridge is approached.

For comparison with a theoretical model, the North Pacific was separated into oceanic provinces of the same age and, to remove the scatter, the values within each province were averaged. The homogeneity and independence of the source data were investigated by comparing the distribution of heat flow within each province with a normal distribution.

The pattern of magnetic anomalies on the ocean floor provides a good estimate of the age of the oceanic crust (Vine 1966; Heirtzler *et al.* 1968). Results from the JOIDES ocean floor sampling programme have established the validity of the magnetic interpretation (Maxwell 1969; McManus & Burns 1969). Further deep-sea drillings in the North Pacific have extended the ocean floor chronology to the upper Jurassic (Scientific Staff, JOIDES Leg VI, 1969).

The North Pacific Ocean was divided into regions of approximately similar age (Fig. 1). From the crest of the East Pacific Rise to anomaly 32, the age of the ocean floor is estimated from the magnetic anomalies. From anomaly 32 to the Marianas Trench, the results of the JOIDES drillings provided the age estimate. The boundaries of the regions shown on Fig. 1 are: The crest of the East Pacific Rise, anomalies 5, 6, 13, and 25, the late/middle Cretaceous, the middle/early Cretaceous, the early Cretaceous/upper Jurassic. Magnetic lineations have been observed to the west of Japan (Uyeda *et al.* 1967) but could not be correlated with the known time scale. This area, which is definitely older than the late Cretaceous, is shown in Fig. 1 and is considered in this study.

Table 1

Statistics of the heat flow distribution in nine provinces of the North Pacific. The number of observations, their mean, standard error and standard deviation are listed for each province. The Kolmogorov–Smirnov $D_{0\cdot1}$ statistic at the 10 *per cent level and the largest observed difference, D_{max}, between sample and population cumulative percentages are also listed.*

Province	n	$\bar{q}$	$\sigma_{\bar{q}}$	s	$D_{0\cdot1}$	D_{max}
Jurassic	14	1·44	0·095	0·357		
and Older	11	1·28	0·059	0·187	44·0	10·0
Early Cretaceous	47	1·18	0·038	0·264	41·0	32·0
Japanese Area	47	1·11	0·032	0·218	47·0	6·0
Middle Cretaceous	60	1·38	0·055	0·427	41·0	20·0
Late Cretaceous	64	1·43	0·066	0·526	34·0	26·0
Anomaly 13–25	59	1·43	0·086	0·662	34·0	14·0
Anomaly 6–13	116	1·61	0·071	0·765	30·0	14·0
Anomaly 5–6	102	2·22	0·107	1·084	27·0	8·0
Anomaly 0–5	65	2·82	0·210	1·696	21·0	12·0

Note: n is the number of heat flow values
$\bar{q}$ is the mean value
$\sigma_{\bar{q}}$ is the standard error of the mean
s is the standard deviation
D is the Kolmogorov–Smirnov statistic

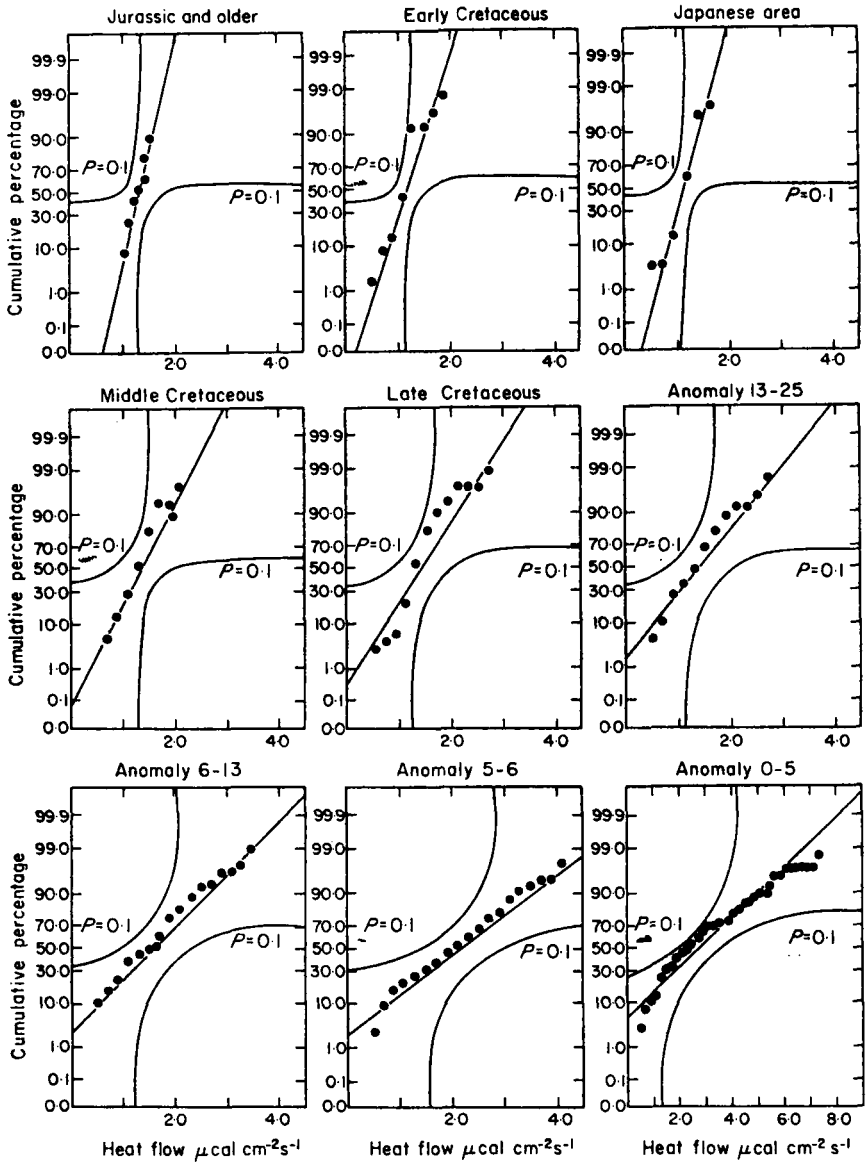

FIG. 3. Graphical test of the hypothesis that the population of heat flow values in each of the nine North Pacific provinces is normal at the 10 per cent level. The cumulative relative frequency is plotted against heat flow value. The theoretical normal curve is indicated by the straight line. The band defines the maximum difference between sample and population cumulative percentages expected 10 per cent of the time (Kolmogorov–Smirnov statistic).

Heat flow data were taken from Lee & Uyeda (1965), Vacquier *et al.* (1966), Vacquier *et al.* (1967), Sclater & Corry (1967), Burns & Grim (1967), Fisher, Von Herzen & Rhea (1967), unpublished data from M. Langseth and R. P. Von Herzen and Sclater *et al.* (1968). Only needle probe measurements showing full penetration or outrigger measurements of fair reliability (six or greater; Langseth, Le Pichon & Ewing 1966) were taken in averaging the data. All values less than $0{\cdot}4\ \mu$ cal cm^{-2} s^{-1} were disregarded as Sclater, Mudie & Harrison (1970) have

shown that measurements this low are almost certainly caused by recent slumping of sediments from surrounding topographic highs. The distributions of heat flow data, satisfying these conditions, for each region of the North Pacific considered, are given in the histograms shown in Fig. 2. Table 1 gives the parameters of these distributions, the mean, standard deviation, standard error, and the estimate of the goodness of fit of these distributions to a normal distribution function. The agreement of distributions in small sampling groups is best estimated by the Kolmogorov–Smirnov statistic (Massey 1951). Fig. 3 presents a cumulative percentage plot of the heat flow values on normal probability paper and gives a graphical test for the null hypothesis that all the samples follow the normal distribution law. As can be seen from Table 1 and Fig. 3, the distribution of heat flow values in provinces of the same age does not contradict a normal distribution law at the 10 per cent level of confidence. Thus, in general, the heat flow values in each region of the same age are homogeneous. This suggests that our method of separation is statistically, as well as geologically, meaningful.

The Jurassic, early Cretaceous, and Japanese provinces have a mean and standard error of $1{\cdot}44 \pm 0{\cdot}095$, $1{\cdot}18 \pm 0{\cdot}038$, and $1{\cdot}11 \pm 0{\cdot}032$ μ cal cm^{-2} s^{-1} respectively. Though the Japanese and early Cretaceous provinces have a mean close to 1·15 and a small standard error, the Jurassic average of 14 values is much greater and has a significantly larger standard error. Three unpublished values of 1·93, 1·89, and 2·20 μ cal cm^{-2} s^{-1} contribute to this mean. As the average of the other 11 values is 1·28 μ cal cm^{-2} s^{-1} with a lower standard error and these three high values are on the border of reliability (only one thermal gradient measured on an outrigger system) we consider the value of $1{\cdot}28 \pm 0{\cdot}059$ μ cal cm^{-2} s^{-1} to be closer to the actual mean heat flow through this area. The distribution of the heat flow in these three areas does not conflict with the hypothesis of normality at the 10 per cent level (Table 1 and Fig. 3).

The middle and late Cretaceous provinces and the region bordered by anomalies 25 and 13 have a mean and standard error of $1{\cdot}38 \pm 0{\cdot}055$, $1{\cdot}43 \pm 0{\cdot}066$, and $1{\cdot}43 \pm 0{\cdot}086$ μ cal cm^{-2} s^{-1} respectively. The Kolmogorov–Smirnov test indicates that the distribution of heat flow in these three areas does not differ significantly from a normal distribution.

The provinces extending from anomaly 13 to the crest of the East Pacific Rise have a mean and standard error of $1{\cdot}61 \pm 0{\cdot}071$, $2{\cdot}22 \pm 0{\cdot}107$, $2{\cdot}82 \pm 0{\cdot}210$ μ cal cm^{-2} s^{-1} respectively. The fit to a normal curve for these three provinces is not in conflict with the observed heat flow observations.

A plot of mean heat flow versus age for the nine regions considered shows a continuous and significant decrease of heat flow from the younger to the older crust (Fig. 4). The histograms of Fig. 2 and the length of the bars on Fig. 4 demonstrate that the scatter in the heat flow values increases from the older to the younger provinces. The continuous decrease in heat flow, away from the crest of the ridge (Fig. 4), is clearly compatible with a model in which hot material is intruded at the crest of the ridge and heat is lost by conduction, as this new crust moves away from the crest.

3. South Atlantic oceanic heat flow

Though reliable heat flow measurements are sparse in the South Atlantic and mostly concentrated around the ridge crest, it is tempting to investigate if the pattern of heat flow in the South Atlantic is similar to that in the North Pacific. The South Atlantic is the only other ocean where the age of the ocean floor is, at present, even partially understood. Deep drilling (Maxwell 1969) in the South Atlantic has con-

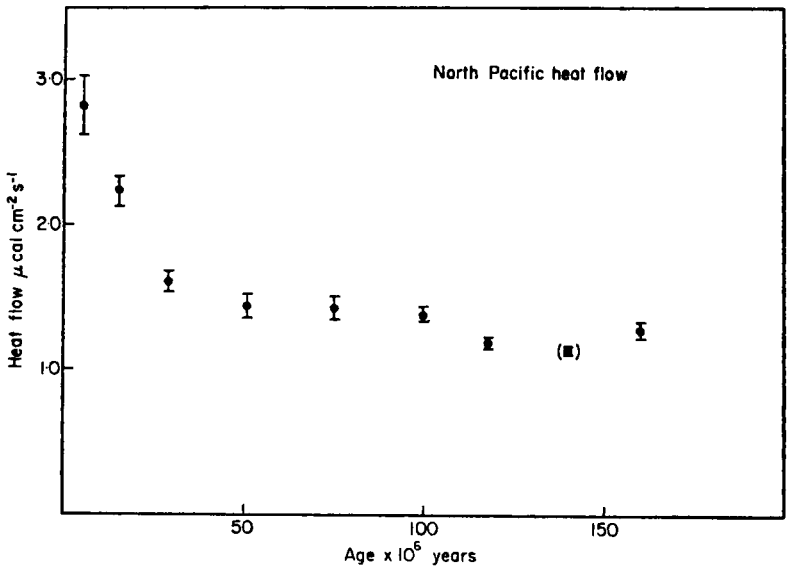

FIG. 4. Plot of mean heat flow against age of province for the North Pacific. The length of the bar gives the magnitude of the respective standard error. The mean value for the youngest province has been plotted for a mean age of 5 My in order to account for the paucity of observations in the crestal regions. An explanation for the lack of values near the crest of the ridge can be found in Oxburgh & Turcotte (1969).

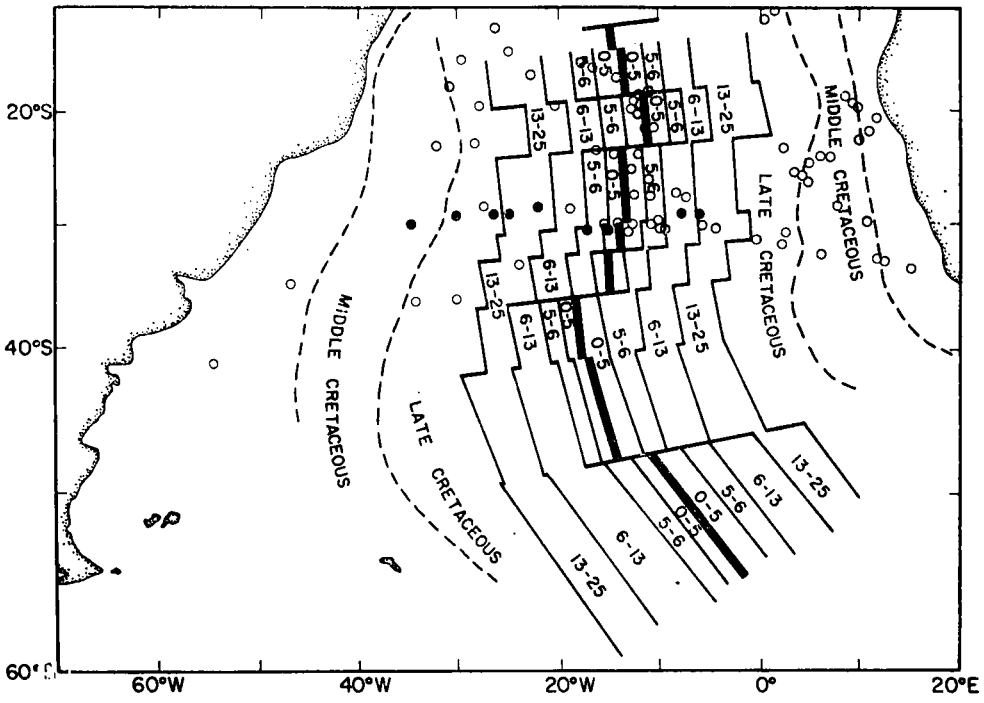

FIG. 5. Provinces of the South Atlantic. The boundaries of the provinces are determined from the magnetic lineations (Dickson *et al.* 1968) and the age of the sediments recovered by JOIDES deep-sea drillings (Maxwell 1969). The thick black line marks the crest of the mid-Atlantic ridge. The open circles are the location of the heat flow measurements and the filled-in circles are the locations of the JOIDES deep-sea drillings.

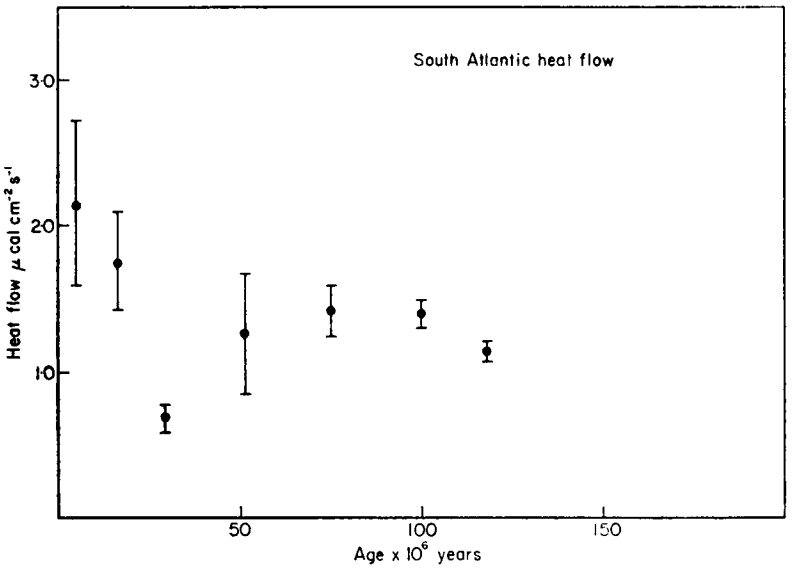

FIG. 6. Plot of mean heat flow against age of province for the South Atlantic. The length of the bar gives the magnitude of the respective standard error. The mean value for the youngest province has been plotted for a mean age of 5 My in order to account for the paucity of observations in the crestal regions. An explanation for the lack of values near the crest of the ridge can be found in Oxburgh & Turcotte (1969).

firmed the age attributed to different parts of the ocean floor by the mapping of the magnetic anomalies (Dickson, Pitman & Heirtzler 1968).

The South Atlantic was separated into provinces of similar age (Fig. 5). The boundaries of these provinces have the same age as those chosen for the North Pacific. The crest of the mid-Atlantic ridge and anomalies 5, 6, 13, and 25 are well defined. The late, middle and early Cretaceous boundaries are determined by assuming a constant spreading rate of 2 cm yr^{-1} (Maxwell 1969) from the present until the early Cretaceous.

Table 2

Statistics of the heat flow distribution in seven provinces of the South Atlantic. The number of observations, their mean, standard error and standard deviation are listed for each province.

Province	n	$\bar{q}$	$\sigma_{\bar{q}}$*	s
Early Cretaceous	7	1·14	0·076	0·164
Middle Cretaceous	13	1·40	0·113	0·361
Late Cretaceous	12	1·42	0·174	0·530
13–25	6	1·26	0·428	0·820
6–13	5	0·69	0·102	0·172
5–6	10	1·75	0·334	0·912
0–5	16	2·15	0·557	2·009

Note: n is the number of heat flow values
$\bar{q}$ is the mean value
$\sigma_{\bar{q}}$ is the standard error of the mean
s is the standard deviation

* The best estimate of the standard error of the mean of a small sample is given by the law of Student–Fisher.

The heat flow data for the South Atlantic were taken from Lee & Uyeda (1965) and Langseth *et al.* (1966). Excepting the low average heat flow value for the province extending from anomaly 6 to 13, the average heat flow decreases with increasing age of the oceanic crust (Fig. 6). This is similar to the pattern shown by the heat flow values in the North Pacific. However, the low number of values precludes a meaningful statistical study of the heat flow distribution within each province. The anomalous value is the average of only five determinations (Table 2). It is not clear that this mean is representative of the heat flow for this province and it was disregarded when fitting theoretical heat flow curves through the average heat flow values for the provinces. The similarity of the heat flow dependence on age for the North Pacific (Fig. 4) and the South Atlantic (Fig. 6) suggests that the heat flow decrease observed in the Pacific may be typical of all oceans.

4. Continental heat flow

Polyak & Smirnov (1968) have analysed in considerable detail the relationship between terrestrial heat flow and the age of the orogenic province where the heat flow was measured. They demonstrate that the heat flow in each province is normally distributed and that the average value decreases with increasing age of the province.

Table 3 lists their data for several orogenic provinces and Fig. 7 presents a plot of the average heat flow values against the age of the corresponding province. The age of the Cenozoic, Mesozoic, Hercynian, and Caledonian orogenies are relatively well known. The Precambrian platforms have been given a rather arbitrary age of 700 My and the shield areas have been ascribed the mean age of the Grenville, of approximately 1100 My. Because a complex multipeak distribution is observed for heat flow values in the Cenozoic, the mean value, 1·78 μ cal cm^{-2} s^{-1}, may not be

Table 3

Heat flow distribution in different continental tectonic provinces (taken from Polyak & Smirnov 1968).

Tectonic provinces	n	q_{min}	q_{max}	$\bar{q}$	$\sigma_{\bar{q}}$	s	Distribution Law
Provinces of Precambrian folding (undifferentiated)	88	0·53	1·33	0·93	0·02	0·17	Normal
Shields	69	0·61	1·32	0·90	0·02	0·15	Normal
Platforms	19	0·53	1·33	1·04	0·05	0·20	Normal
Provinces of Caledonian folding	17	0·68	1·71	1·11	0·07	0·28	Normal
Provinces of Hercynian folding	60	0·60	1·90	1·24	0·03	0·25	Normal
Provinces of Mesozoic folding and activation	26	1·00	2·12	1·42	0·06	0·31	Normal
Provinces of Cenozoic folding and activation							
Foredeeps and intermontane troughs	55	0·52	1·58	0·98	0·03	0·24	Normal
Folded mountain structures of migeosynclinal zones	19	1·20	2·20	1·75	0·06	0·25	Normal
Zones of Cenozoic volcanism	55	1·20	3·49	2·20	0·06	0·42	Normal
Continental rift zones:							
Nyasa	20	—	—	1·00	—	—	Unknown
Baikal	11	1·21	3·40	2·40	0·18	0·59	Unknown

Note: n is the number of heat flow values
$\bar{q}$ is the mean value
$\sigma_{\bar{q}}$ is the standard error of the mean
s is the standard deviation

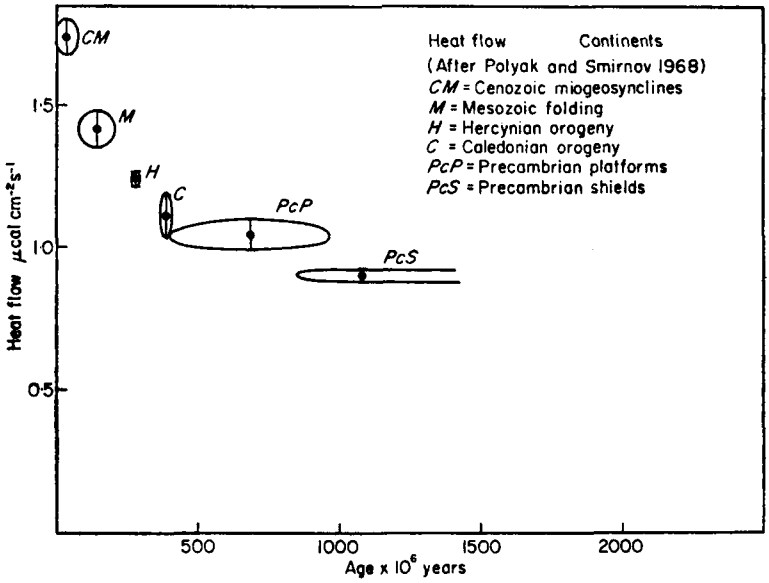

FIG. 7. A plot of mean heat flow against age of orogenic province for continents (after Polyak & Smirnov 1968; Smirnov 1968, Fig. 1).

representative of the mean flow through this province (Polyak & Smirnov 1966). The mean heat flow through the orogenic provinces decreases from 1·42 μ cal $cm^{-2} s^{-1}$ for the Mesozoic to 0·90 μ cal $cm^{-2} s^{-1}$ for the Precambrian shields. The small standard deviation of the values for the Precambrian and the exponential nature of the decrease on Fig. 7 suggest that, in this province, the heat flow may be close to an equilibrium value.

There is some indication that the mean values of all heat flow measurements on land may have to be raised. Simmons & Nur (1968) compared the physical properties of granite *in situ* measured in two boreholes with those from laboratory measurements on dry samples. The correction for the effect of cracks and saturation with water on the thermal conductivity measurements could raise the average heat flow in all continental areas by as much as 10–15 per cent. When this correction is applied, the mean for the shield areas becomes 1·0 to 1·05 μ cal $cm^{-2} s^{-1}$. This value is very close to the average heat flow observed on the older portions of the oceanic crust.

5. Equality of continental and oceanic heat flow

The mean heat flow through the deep-ocean crust is approximately equal to the mean flow through the continents (Lee & Uyeda 1965; Polyak & Smirnov 1968). Bullard (1952) proposed two alternative hypotheses in explanation: First, that the oceanic heat flow is due to convection; second, that, to a first approximation, the mean chemical composition of the mantle is the same over both continents and oceans when averaged down to depths of several hundred kilometres. The second hypothesis was the more popular and led to several geochemical models of the upper mantle (Ringwood 1958; McDonald 1963; Clark & Ringwood 1964).

Several authors (Langseth *et al.* 1966; McKenzie 1967; McKenzie & Sclater 1969; Sleep 1969) have demonstrated that, in a sea-floor spreading model, a considerable proportion of the heat lost by the oceans is due to the creation of oceanic

lithosphere. Thus, there is no longer any necessity to assume that the mean radioactive composition beneath continents and oceans, when averaged down to considerable depths, are identical.

The mean heat flow in any continental or oceanic province is strongly related to the age of the province (Figs 4 and 7). However, the time scales for the thermal decay of the heat flow for the two realms are an order of magnitude different. The continents take a billion years to reach a constant value of $1{\cdot}00\ \mu$ cal cm^{-2} s^{-1} while the oceans reach a value of $1{\cdot}1\ \mu$ cal cm^{-2} s^{-1} after only 100 My. The continental and oceanic crustal rocks have a radically different chemical composition. This and the different time scales of the heat flow decay suggest that the processes responsible for the observed distribution of heat flow differ for continents and oceans. Although the mean heat flow through the two regions is the same, the strong dependence of heat flow on age (Figs 4 and 7) suggest that this equality may be entirely fortuitous and need not necessarily be related to a deep-seated mantle process. Thus, a comparison of the gross means is not a meaningful method of evaluating the contribution from the deep interior of the Earth. It is more pertinent to examine the significance of the strong dependence of heat flow on age for both the oceanic and continental values and to pay special attention to the values in the older provinces. These values may be close to equilibrium and hence enable a better estimate to be made of the heat flow from the upper mantle in both cases.

The problems are then to account for (a) the dependence of heat flow on age, and (b) the approximate equality of the heat flow through the shield areas with that through the oldest portions of the deep oceans. We will consider the geochemical models of the crust and upper mantle of the continents proposed by Roy, Blackwell & Birch (1968) and oceans proposed by Clark & Ringwood (1964) and Ringwood (1969; Fig. 5). Heat lost in the creation of oceanic lithosphere will play a significant role in the contribution to the oceanic heat flow (McKenzie 1967; McKenzie & Sclater 1969).

6. Heat flow on continents

Continental heat flow values are a function of the age of the latest thermal event, the intensity of this event and the concentration of radioactive elements below the continents. An estimate of the vertical distribution of these elements has come from recent work by Birch, Roy & Decker (1968), Roy, Blackwell & Birch (1968), and Lachenbruch (1968). These authors have separated North America into five major thermal regions and have shown that within each region the heat flow values show a striking linear correlation with the concentration of radioactive elements in the surface rocks. To investigate whether the data for North America show a strong correlation with age and to compare the thermal regions of Roy *et al.* (1968) with the tectonic provinces of Polyak & Smirnov (1968) we superimposed all available North American heat flow data (Lee & Uyeda 1965; Roy *et al.* 1968; Blackwell 1969) upon a tectonic map of North America (King 1969; Fig. 8). The two youngest provinces were separated according to the most recent thermal event. The Cenozoic is the Basin and Range province of Blackwell (1969) and the Mesozoic is, for the most part, the area of western North America folded in the Mesozoic and not affected by younger tectonic activity. Except for H (the mean of six values in the southern Appalachians) the data for North America (Fig. 9, Table 4) are remarkably similar to those presented by Polyak & Smirnov (1968; Fig. 7). Hamza & Verma (1969) have compiled radioactive age determinations and heat flow measurements for Africa, Australia and India. They suggest that the decrease of heat flow with age is true for all continents.

The two oldest thermal regions of Roy *et al.* (1968), the Central Stable region and the New England area, correspond to the Precambrian Platforms (PcP) and

Caledonian (*C*) provinces respectively (Fig. 8). These authors have shown that the heat flow and surface radioactivity data for these two provinces plot on the same straight line (Fig. 10). Roy (personal communication) has further shown that two published values (Hyndman, *et al.* 1968) and one unpublished value for the Australian shield, and three unpublished values for the Canadian shield also fall on this line (Fig. 10). This linear relationship affords a simple explanation of the heat flow in the Caledonian and older provinces. The slope of the line gives a measure of the

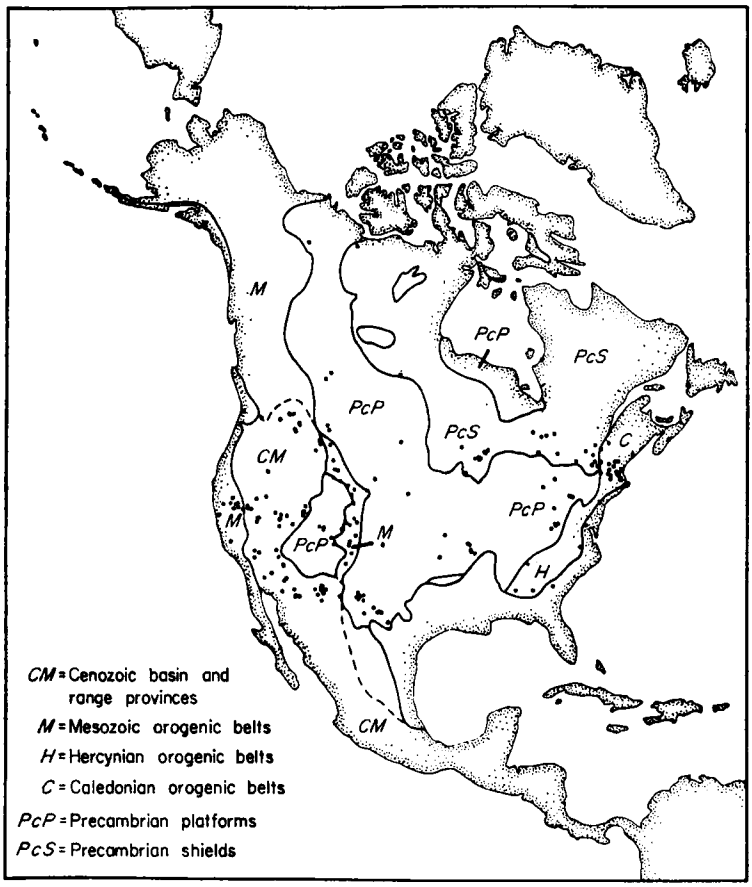

FIG. 8. Tectonic map of North America, after King (1969) The black dots represent heat flow measurements.

thickness of the radioactive layer and the intercept gives the heat flow from below. For these three provinces the variation of heat flow can be explained by assuming an 8-km thick radioactive layer with a uniform heat flow of $0{\cdot}8\mu$ cal cm^{-2} s^{-1} at its base. The decrease in heat flow from the Caledonian to the shields can be explained by the reduction of radioactivity in the surface layer. There is no need to invoke any thermal energy due to intrusion. Thus, the intercept heat flow may represent the equilibrium flux from the lower crust and upper mantle.

It is supposed that the continental rocks have differentiated from the underlying mantle and that, in the course of this differentiation, the uranium, thorium and potassium are selectively removed from the mantle and are concentrated at high levels in the crust by magmatism. For the Cenozoic province, it is likely that the thermal energy due to magmatism is responsible for a large fraction of the surface heat flow. The decay of this heat flow is a function of the age of emplacement, the size of the magmatic body, the degree of metamorphism and the impoverishment of

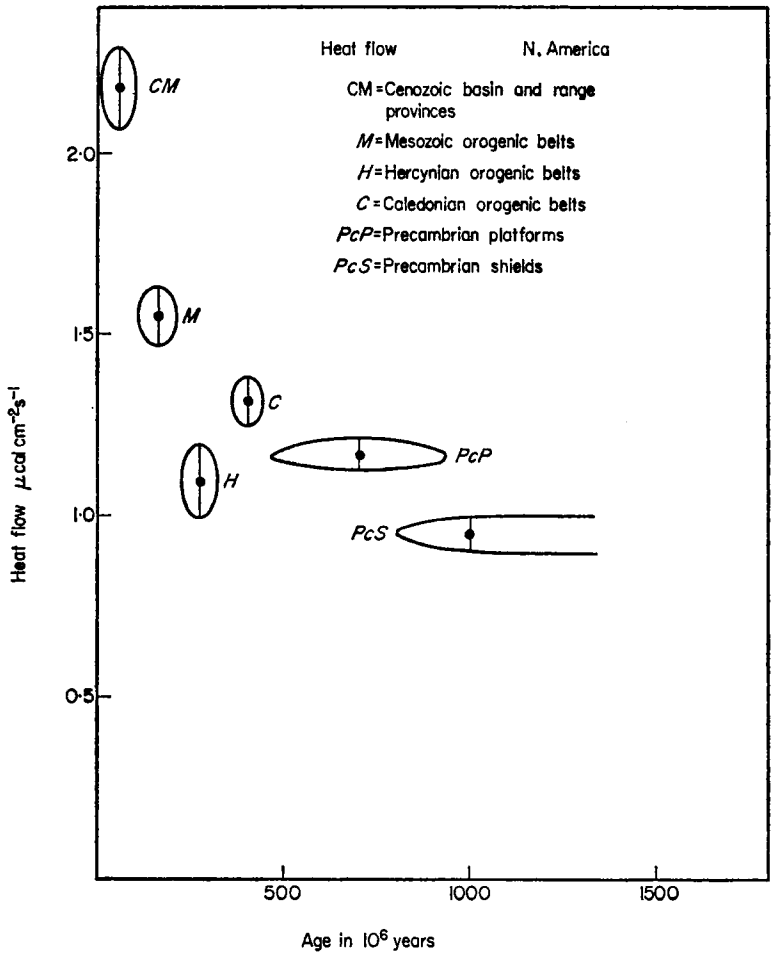

FIG. 9. A plot of mean heat flow against age of last thermal event for North America.

the radioactive elements. From the explanation of Roy *et al.* (1968) for Fig. 10 one can infer that all energy of intrusion has been lost after 400 million years. If radioactive studies on rocks of Mesozoic age yield the same high radioactive concentrations as those reported by Birch *et al.* (1968) for the White Mountains, the rest of the Mesozoic values would plot on the line of Roy *et al.* (1968; Fig. 10) and would imply that the time scale of the decay of the intrusive energy could be as short as 200 million years. However, there are few reported measurements to substantiate these high

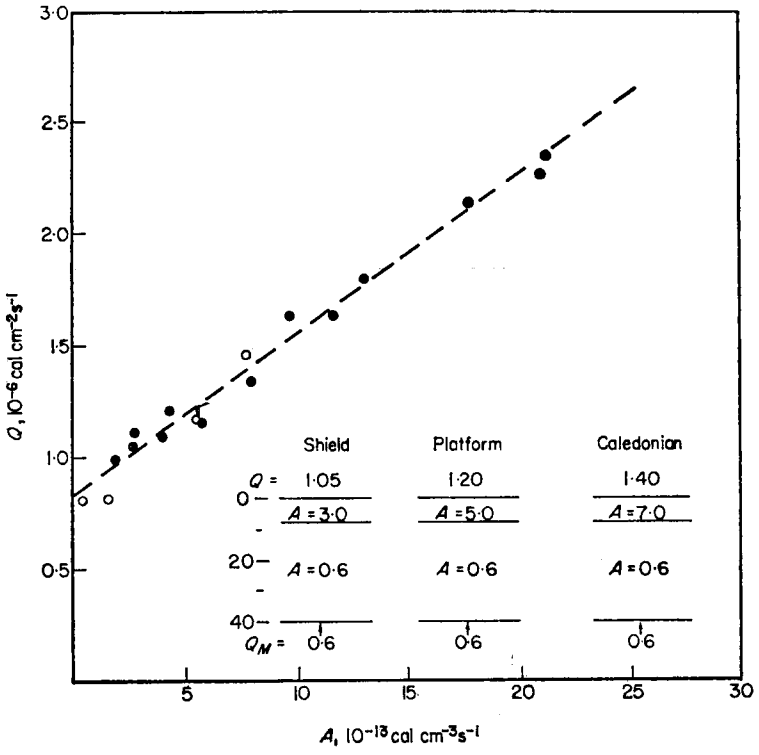

FIG. 10. Heat flow and heat productivity data for plutons in the New England area (solid circles), the Central Stable region (open circles) and the Australian and Canadian shields (open circles with crosses). The sections represent steady state models of the crust compatible with the data (Roy *et al.* 1968; Hyndman *et al.* 1968; Roy, personal communication). The three highest values are from the White Mountains, of Mesozoic age, and have not been considered in evaluating a mean radioactivity for the Caledonian surface layer.

Table 4

Heat flow distribution for the different continental tectonic provinces of North America

Tectonic provinces	n	q_{min}	q_{max}	$\bar{q}$	$\sigma_{\bar{q}}$	s	$D_{0.1}$	D_{max}	Distribution Law
Provinces of Precambrian folding									
Undifferentiated	63	0·44	1·90	1·09	0·032	0·253			
Shields	22	0·69	1·32	0·95	0·038	0·179	25·0	13·0	Normal
Platforms	41	0·44	1·90	1·17	0·040	0·254	19·1	10·1	Normal
Provinces of Caledonian folding	17	0·81	1·80	1·31	0·070	0·290	28·6	12·0	Normal
Provinces of Hercynian folding	6	0·73	1·40	1·09	0·093	0·229	47·0	14·0	Normal
Provinces of Mesozoic folding and activation	34	0·62	2·28	1·55	0·081	0·470	21·0	9·0	Normal
Provinces of Cenozoic folding and activation	63	1·10	6·89	2·18	0·100	0·795	15·4	16·5	Unknown

Note: n is the number of values; $\bar{q}$ is the mean value; $\sigma_{\bar{q}}$ is the standard error of the mean; s is the standard deviation; D is the Kolmogorov–Smirnov statistic; all values are in μ cal cm^{-2} s^{-1}.

concentrations. Lachenbruch (1968) has shown that a model where the radioactive concentrations of the crustal rocks decrease logarithmically with depth can explain the linear relationship of heat flow to radioactivity found for the provinces older than the Caledonian. Such a model might reflect a continuous history of fractional melting in the mantle resulting in a strong upward differentiation of the lighter elements (Ringwood 1969). One could then qualitively account for the decrease of the mean surface radioactivity with increasing age by two main factors: (a) The decay of the radioactive elements themselves, particularly potassium; and (b) the erosion of the logarithmic layer.

For a comparison with the heat flow through the old ocean basins we will consider the regional flow through the shield areas as this value is close to the equilibrium and hence sets a lower limit to temperatures in the mantle. Our model which is compatible with the data of Roy *et al.* (1968) consists of a two-layer crust. The upper

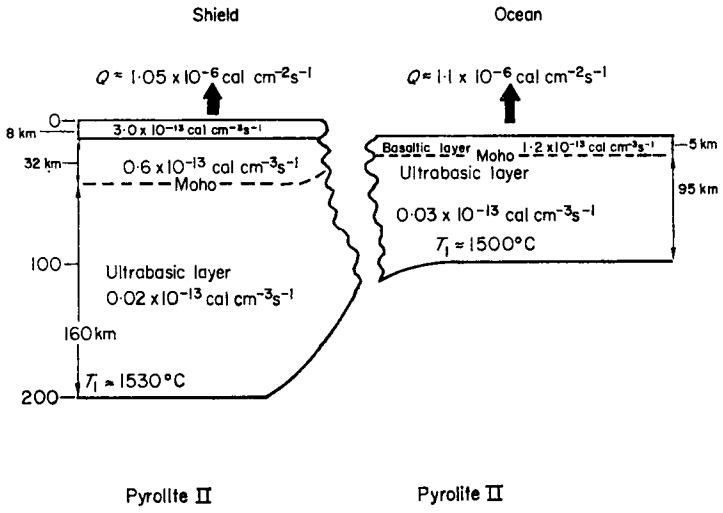

FIG. 11. Geochemical model of continental shield and oceanic lithosphere (after Fig. 5 of Ringwood 1969) assuming convection maintains a constant temperature at the base of the two lithospheres. A mean conductivity of $7{\cdot}1 \times 10^{-3}$ cal cm^{-1} s^{-1} °C^{-1} and adiabatic gradient of 0·3 °C km^{-1} have been assumed.

layer, where measurements of radioactivity have been made, is 8 km thick and contributes 0·25 μcal cm^{-2} s^{-1} to the surface heat flow; the lower layer is assumed to have a radioactive concentration of $0{\cdot}6 \times 10^{-13}$ cal cm^{-3} s^{-1} and contributes only 0·2 μcal cm^{-2} s^{-1} to the surface flux. Below this crust, Ringwood's (1969) model consists of a chemically zoned upper mantle with a refractory dunite-peridotite layer overlying primitive pyrolite (Fig. 11). Brune & Dorman (1963) have suggested that there may exist a low velocity zone at a depth of approximately 200 km beneath the shield areas. If the lower ultrabasic layer indeed consists of dunite-peridotite with a mean radioactive heat production of $0{\cdot}02 \times 10^{-13}$ cal cm^{-3} s^{-1} (Holmes 1965; p. 1002), then the total heat contribution of this layer is 0·03 μcal cm^{-2} s^{-1}. Thus, in the model we have chosen, the lithosphere comprising the Precambrian shields contributes 0·48 μcal cm^{-2} s^{-1} to the surface heat flow. This leaves a heat flow of approximately 0·6 μcal cm^{-2} s^{-1} coming from below the lithosphere.

7. Oceanic heat flow

Heat flow observations in the North Pacific and South Atlantic show a systematic decrease of mean heat flow with increasing age of the ocean floor. Such a decrease is expected in the sea-floor spreading hypothesis where all hot material is being intruded at the crest of the ridges. Langseth *et al.* (1966), McKenzie (1967) and Langseth & Von Herzen (in press) have computed the heat flow resulting from the cooling of a slab of lithosphere moving away from the ridge axis. Models with a slab thickness of 50–100 km and a basal temperature of 550°–1200 °C have given reasonable fits to the observed heat flow data. The problem of preserving the equality of the heat flow through shields and older ocean basins when oceanic and continental plates are permitted to move has not been considered in these models (Bullard 1968). To explain this equality, within the framework of plate tectonics, it is necessary to examine the lower boundary condition and the possible heat contribution of the oceanic lithosphere. The lower boundary condition can be set on either temperature or heat flow.

As the temperature structure of the mantle is not very different from adiabatic, it is reasonable to assume that the low velocity layer is nearly isothermal. Such a state is easily maintained if convective processes are efficient. Thus, the temperatures at the base of the oceanic and continental lithospheres can be considered roughly equal. If this is so, and heat sources contribute 0·48 μ cal cm^{-2} s^{-1} to the heat flow through the shields, then the approximate equality of heat flow through shields and old ocean basins is a consequence of the lithosphere being twice as thick beneath the shields (Fig. 11). In this model the oceanic lithosphere is depleted in radioactive elements. The low radioactivity is consistent with measurements made on lherzolites, rocks recovered from the ocean floor (Wakita *et al.* 1967; Table 5). As the base of both lithospheres have nearly the same temperature, no difficulty is encountered in preserving the heat flow equality while moving the plates. In this model, the composition of the mantle is the same under both continents and oceans.

An alternative way to explain the equality of heat flow when allowing for plate movements is to assume that the heat flowing through the base of the two lithospheres is approximately equal. This demands that the oceanic lithosphere carry a significant component of the surface heat flow, roughly 0·4 μ cal cm^{-2} s^{-1}, along with it. The

Table 5

Average abundances of heat-producing elements and heat production from radioactivity in possible rocks of the oceanic lithosphere.

	Average abundances of the radioactive elements in grams per 10^6 grams of rock			Heat production from radioactivity in calories per year per 10^6 grams of rock					
								per 10^6 cm^3	in calories per second per cm^3
Rock groups	U	Th	K^{40}	U	Th	K^{40}	Total	Total	Total
Basaltic rocks (Holmes 1965)	0·7	3·0	1·1	0·5	0·6	0·2	1·30	3·80	$1·20\times10^{-13}$
Ultrabasic rocks (Holmes 1965)	0·013	0·05	0·001	0·01	0·01	0·0002	0·02	0·07	$0·02\times10^{-13}$
Lherzolites (Wakita *et al.* 1967)	0·019	0·05	0·007	0·02	0·01	0·0014	0·03	0·10	$0·03\times10^{-13}$
Pyrolite I	0·189	0·79	0·28	—	—	—	—	—	$0·32\times10^{-13}$
Pyrolite II (after Ringwood 1958)	0·059	0·25	0·09	—	—	—	—	—	$0·10\times10^{-13}$

material comprising the lithosphere would then be considerably more radioactive than common ultrabasic rocks. In the geochemical models of Ringwood (1969) and Clark & Ringwood (1964), the parental material is pyrolite from which are derived the basaltic and ultrabasic rocks. If the basaltic layer of the oceanic crust is 5 km thick (layer 2 and layer 3), then the underlying ultrabasics (lherzolite?) may be as much as 15 km thick. A mixture of one part basalt with three parts ultrabasic gives pyrolite with a radioactive heat generation of $0{\cdot}32 \times 10^{-13}$ cal cm^{-3} s^{-1} (Table 5). To obtain a heat flow of 0·4 μ cal cm^{-2} s^{-1} from the oceanic lithosphere, one has to choose a plate thickness of 120 km comprised of the following layers: Five kilometres of basalt with a radioactive heat production of $1{\cdot}2 \times 10^{-13}$ cal cm^{-3} s^{-1}, 15 km of ultrabasic (lherzolite) with a heat production of $0{\cdot}03 \times 10^{-13}$ cal cm^{-3} s^{-1} and 100 km of pyrolite with a heat production of $0{\cdot}32 \times 10^{-13}$ cal cm^{-3} s^{-1}. This plate rests on a more primitive pyrolite with a mean heat production of $0{\cdot}1 \times 10^{-13}$ cal cm^{-3} s^{-1} down to a depth of 400 km (Fig. 12). These values for the heat production are consistent with Clark & Ringwood's (1964) proposal that under the oceans there is a uniform gradient of heat generation for pyrolite from $0{\cdot}35 \times 10^{-13}$ cal cm^{-3} s^{-1} at the base of the Moho to $0{\cdot}007 \times 10^{-13}$ cal cm^{-3} s^{-1} at a depth of 400 km.

This model of an ocean basin adjoining a shield area is shown in Fig. 12. The contribution of the oceanic lithosphere to the surface heat flow is 0·4 μ cal cm^{-2} s^{-1}. This leaves 0·7 μ cal cm^{-2} s^{-1} coming from below the lithosphere. At a depth of 200 km, the heat flow from below is approximately 0·6 μ cal cm^{-2} s^{-1}. This value is similar to that at a depth of 200 km under the shields. As in the first model the

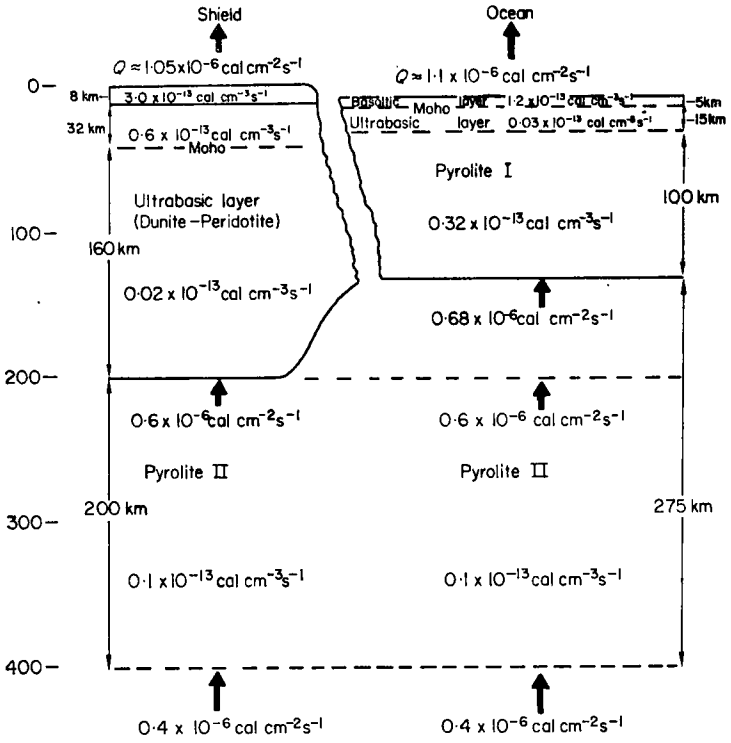

FIG. 12. Models of continental shield and oceanic lithosphere (based on Clark & Ringwood 1964) assuming a constant heat flux at a depth of 200 km. The thick arrows indicate the heat flow at different levels

composition of the mantle at the base of the lithosphere under both continents and oceans is the same and plate movements will not alter the heat flow.

Talwani *et al.* (1968) have observed essentially a zero free air gravity anomaly over oceanic ridges. This suggests that the lithosphere is isostatically compensated and that the relief of the ridge may be accounted for by thermal expansion of the lithosphere (McKenzie & Sclater 1969). The questions remain as to whether (a) the production of oceanic lithosphere can explain satisfactorily both the observed heat flow and topographic relief of ridges, and (b) the observations give clear support for one or other of the geochemical models.

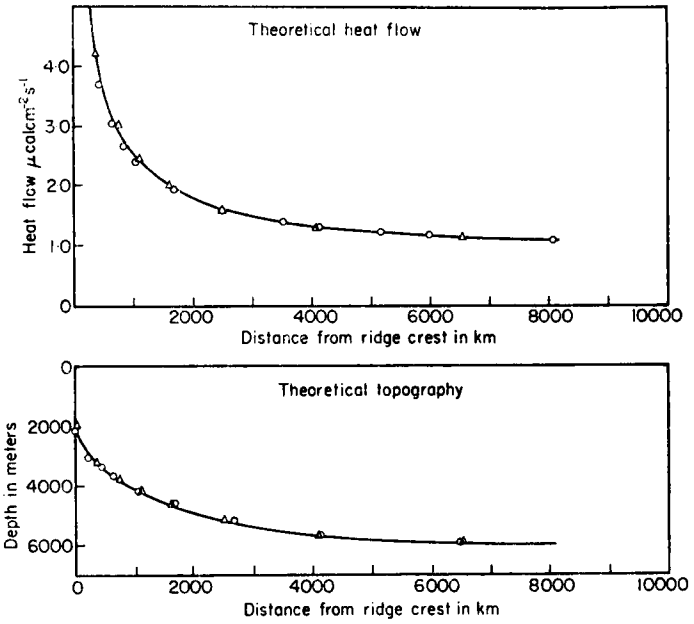

FIG. 13. Comparison of theoretical models of heat flow and topography showing the effect of varying the radioactive content of the lithosphere.

/ $L = 100$ km, $T_1 = 1475$ °C, $K = 7{\cdot}12 \times 10^{-3}$ cal °C^{-1} cm^{-1} s^{-1}, $V = 5$ cm yr^{-1}, $H = 0{\cdot}1 \times 10^{-13}$ cal cm^{-3} s^{-1}, $\Delta_C = 0{\cdot}3$ °C km^{-1}

△ $K = 7{\cdot}46 \times 10^{-3}$ cal °C^{-1} cm^{-1} s^{-1}, $H = 0{\cdot}0 \times 10^{-13}$ cal cm^{-3} s^{-1}, other parameters as above

○ $K = 6{\cdot}37 \times 10^{-3}$ cal °C^{-1} cm^{-1} s^{-1}, $H = 0{\cdot}32 \times 10^{-13}$ cal cm^{-3} s^{-1}, other parameters as above

8. Properties of the models

The model of the oceanic lithosphere used here is similar to the one described by McKenzie (1967). A plate of constant thickness is produced on a vertical boundary at the ridge axis and moves away at a constant velocity. The solution for the temperature structure within the lithosphere, the surface heat flow and the elevation can be found in Appendix I. The radioactive heat production term was kept in the heat flow equation and an adiabatic gradient of temperature, 0·3 °C km^{-1}, was specified for the vertical boundary beneath the ridge axis. At the base of the lithosphere, the temperature is that of incipient melting of pyrolite at that depth and is

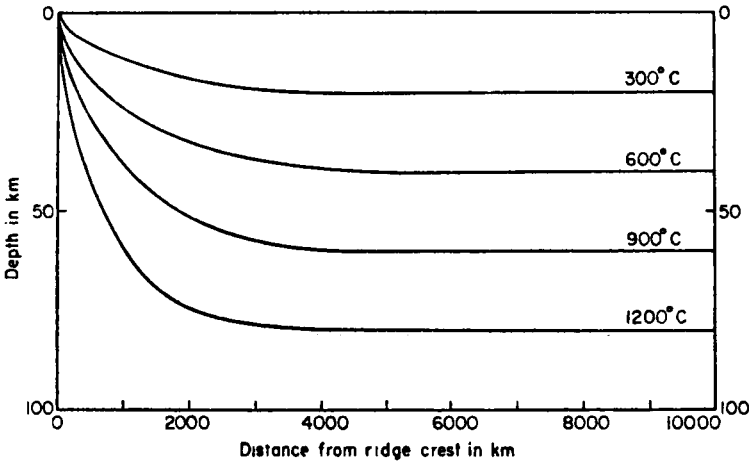

FIG. 14. Isotherms under the North Pacific. The lithosphere of thickness 100 km is moving at 5 cm yr^{-1} to the right.

obtained from the solidus/liquidus curve of pyrolite (Green & Ringwood 1967; Fig. 12). This curve has a gradient of approximately 10 °C kb^{-1}. Once the thickness of the slab is assumed, the temperature is then completely determined. The thermal conductivity is the least well known of all the parameters controlling the temperature of the lithosphere. For the models considered in this paper, once the thickness (and hence the temperature) and radioactive heat production are assumed, the mean conductivity of the lithosphere is defined uniquely by the condition of a uniform heat flow of 1·1 μ cal cm^{-2} s^{-1} observed at great distances from the crest of the ridge. If a different temperature were assigned to the base of a slab of the same thickness, the conductivity would vary so as to retain a constant value for $K(T_1 - T_0)$. With these boundary conditions a small variable radioactive heat production term has no significant effect on either the heat flow anomaly or the elevation (Fig. 13). This arises from fixing the temperature at the base of the slab and demanding that the conductivity be lowered when the radioactivity is increased. Because of this lack of sensitivity to the radioactive content, one is free to choose any internal heat generation term in the range $0\text{–}0{\cdot}32 \times 10^{-13}$ cal cm^{-3} s^{-1}. In the models used to compare theoretical curves with the observed heat flow and topography, a value of $0{\cdot}1 \times 10^{-13}$ cal cm^{-3} s^{-1} has been assumed. Such a value is consistent with a model of oceanic lithosphere where a basaltic layer overlies a thick ultrabasic lid (Fig. 11 and Ringwood 1969, Fig. 5). The isotherms within an oceanic lithosphere 100 km thick moving at 5 cm yr^{-1} are shown in Fig. 14.

9. Oceanic heat flow and the topography of ridges

The North Pacific is the only ocean where there are enough heat flow observations to enable a meaningful comparison between the theoretical profiles and the observed heat flow and topography. The theoretical heat flow is strongly dependent on the assumed velocity of spreading. Examination of linear magnetic anomalies in the North Pacific reveals that the spreading rate varies from 4 cm yr^{-1} for the two provinces near the ridge crest to 5 cm yr^{-1} for the provinces extending from anomaly

6 to 32. The age of the sediment recovered in recent deep drillings in the Northwest Pacific (Scientific Staff, Leg VI, 1969) suggests that the spreading rate could have varied from 7 cm yr^{-1} in the late Cretaceous to 9 cm yr^{-1} in the Jurassic (Fig. 1). Because of this large change in spreading rate one should not expect to be able to match the observed heat flow with a curve based on a single spreading rate.

The heat flow and topography due to slabs of lithosphere 75, 100 and 125 km thick, moving at a velocity of 5 cm yr^{-1} are compared with observed heat flow averages in the North Pacific and an east–west topographic profile at 20° N (Udintsev 1964) (Fig. 15).

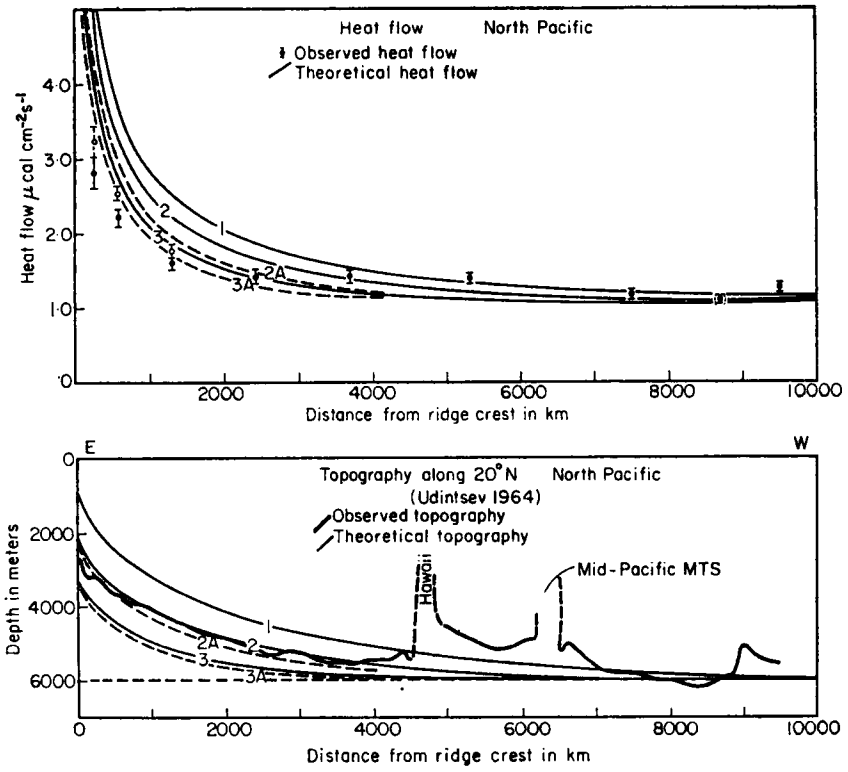

FIG. 15. (a) Comparison of observed heat flow averages in the North Pacific with five theoretical profiles. (b) Comparison of observed topography (Udintsev 1964) with five theoretical profiles. L is the thickness of the lithosphere, T_1 is the basal temperature, K is the thermal conductivity, v is the half spreading rate of the slab, H is the rate of internal heat generation and Δ_c is the adiabatic temperature gradient. The open circles represent an increase of 15 per cent in the heat flow for the three provinces close to the crest of the ridge.

1 $L = 125$ km, $T_1 = 1550$ °C, $K = 8{\cdot}36\times10^{-3}$ cal °C^{-1} cm^{-1} s^{-1}, $V = 5$ cm yr^{-1}, $H = 0{\cdot}1\times10^{-13}$ cal cm^{-3} s^{-1}, $\Delta_c = 0{\cdot}3\times10^{-5}$ °C cm^{-1}

2 $L = 100$ km, $T_1 = 1475$ °C, $K = 7{\cdot}12\times10^{-3}$ cal °C^{-1} cm^{-1} s^{-1}, other parameters as in 1

2A $L = 100$ km, $T_1 = 1475$ °C, $K = 7{\cdot}12\times10^{-3}$ cal °C^{-1} cm^{-1} s^{-1}, $V = 4$ cm yr^{-1}, other parameters as in 1

3 $L = 75$ km, $T_1 = 1400$ °C, $K = 5{\cdot}68\times10^{-3}$ cal °C^{-1} cm^{-1} s^{-1}, $V = 5$ cm yr^{-1}, other parameters as in 1

3A $L = 75$ km, $T_1 = 1400$ °C, $K = 5{\cdot}68\times10^{-3}$ cal °C^{-1} cm^{-1} s^{-1}, $V = 4$ cm yr^{-1}, other parameters as in 1

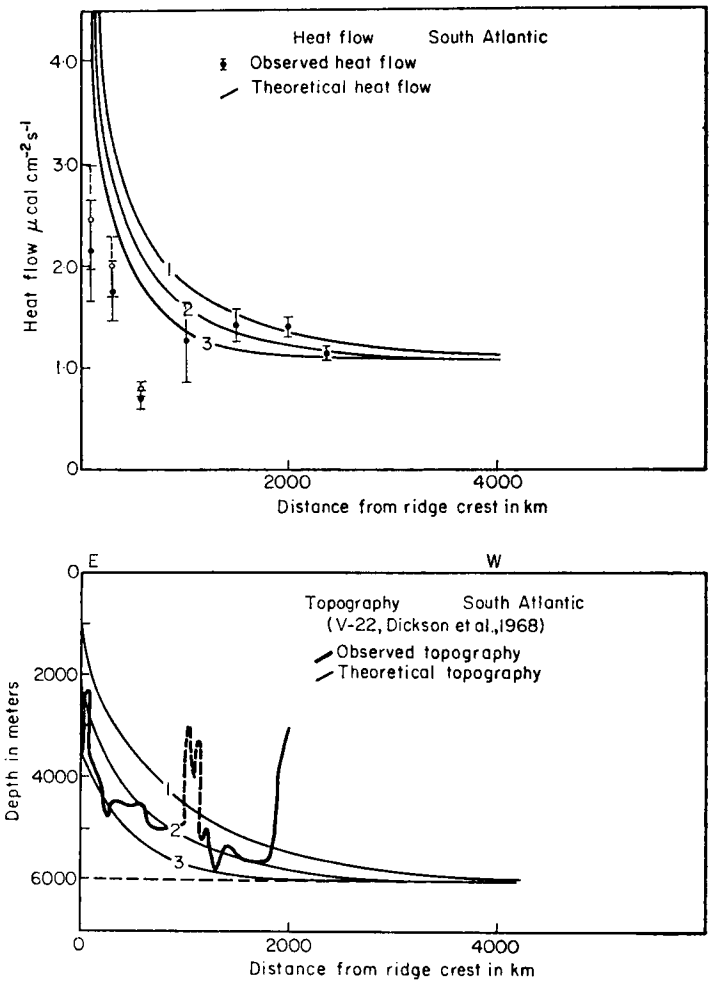

FIG. 16. (a) Comparison of observed heat flow averages in the South Atlantic and three theoretical profiles. (b) Comparison of observed topography in the South Atlantic V-22 (Dickson *et al.* 1968) and three theoretical profiles. Symbols are defined in Appendix I and the caption of Fig. 15.

1 $L = 125$ km, $T_1 = 1550$ °C, $K = 8{\cdot}36 \times 10^{-3}$ cal °C^{-1} cm^{-1} s^{-1}, $V = 2$ cm yr^{-1}

2 $L = 100$ km, $T_1 = 1475$ °C, $K = 7{\cdot}12 \times 10^{-3}$ cal °C^{-1} cm^{-1} s^{-1}, $V = 2$ cm yr^{-1}

3 $L = 75$ km, $T_1 = 1400$ °C, $K = 5{\cdot}68 \times 10^{-3}$ cal °C^{-1} cm^{-1} s^{-1}, $V = 2$ cm yr^{-1}

In regions of rough topography the heat flow average may be biased on the low side. Sclater, Mudie & Harrison (1970) have shown that, in a small region of high topographic relief on the Hawaiian Arch, the preferential positioning of heat flow measurements in sediment ponds yielded an average heat flow for the small region that was 30 per cent lower than the mean for the whole Arch. A systematic heat flow survey at right angles to the Galapagos rift zone yielded a mean of 5·0 μcal cm^{-2} s^{-1} for 18 heat flow observations within a 100 km wide zone about the spreading centre

(Piquero 7, unpublished). These two results suggest that the average heat flow in regions of rough topography may have to be raised. To correct for this possible bias, the average for the younger provinces has been increased by a conservative 15 per cent and shown as open circles in Fig. 15.

The theoretical elevations for 75- and 125-km thick lithospheres effectively bracket the observed topography (Fig. 15). A slab of lithosphere 100 km thick with a basal temperature of 1475 °C spreading at 5 cm yr^{-1} gives a reasonable fit to the topographic section along 20° N. There is strong experimental (Sclater *et al.* 1970) and theoretical (Oxburgh & Turcotte 1969) evidence that we have underestimated the bias in heat flow for the crestal zone. If the lowering of the heat flow is as much as 50 per cent for the provinces close to the crest, a slab, 100 km thick, moving at 4 cm yr^{-1} would give a theoretical anomaly consistent with the heat flow observations near the crest of the ridge. Further from the ridge, the curve for a spreading rate of 5 cm yr^{-1} would adequately account for the data. A combination of the two spreading rates for a lithosphere 100 km thick would then give a reasonable fit to the observed heat flow. As the theoretical topographic profile is less sensitive to changes in spreading rate, this model would also fit the topographic data. Differences in spreading rate have little effect on the tail of the theoretical profiles (Fig. 15). Thus, it is not necessary to compute a curve of the expected heat flow and topography for the faster spreading in the older regions. A point of interest is that in the region comprising the Hawaiian chain and the mid-Pacific mountains the anomalous topography is accompanied by a heat flow slightly higher than that in the surrounding deep ocean basins.

An attempt is made to explain the heat flow and topographic relief in the South Atlantic (Fig. 16). In this ocean, the spreading rate has been roughly constant since the early Cretaceous (Maxwell 1969). A model of oceanic lithosphere 100 km thick would adequately explain the topographic profile V-22 (Dickson *et al.* 1968). This profile was chosen because it is long, south of the heavily sedimented Argentine Basin and it does not cross either the Walvis or Rio Grande Ridges. The scatter in the observed heat flow in each province and the possible bias of the heat flow average in the regions of rough topography prevent us from selecting a model of lithosphere from the heat flow measurements. It is encouraging that a good fit to the ridge topography is obtained by taking the same model of the lithosphere as that for the North Pacific. Further, the theoretical topography has the same basal depth of 6000 m in both oceans. This suggests that the model for the Pacific may be valid for all oceans.

10. Discussion of the oceanic model

Because of the uncertainty in the thermal conductivity, a model of lithosphere in which a small amount of radioactive heat generation is assumed cannot be separated from one which is totally depleted in heat producing elements. However, the two models which were suggested to explain the equality of heat flow through the shields and old oceans would have different chemical compositions. A lithosphere which contributes significantly to the surface heat flow is likely to have a composition close to that of pyrolite with a thin lid of ultrabasic and basaltic rocks. Within the framework of plate tectonics, where the lithosphere is envisaged as the lowest melting fraction of the upper mantle, this model implies a two-stage differentiation process with increasing enrichment in the lighter elements. Pyrolite II is the parent of pyrolite I which in turn gives rise to the basaltic and ultrabasic layers. A depleted lithosphere consisting mainly in ultrabasics can be derived directly from the more primitive pyrolite II. The differentiation history of such a model is simpler.

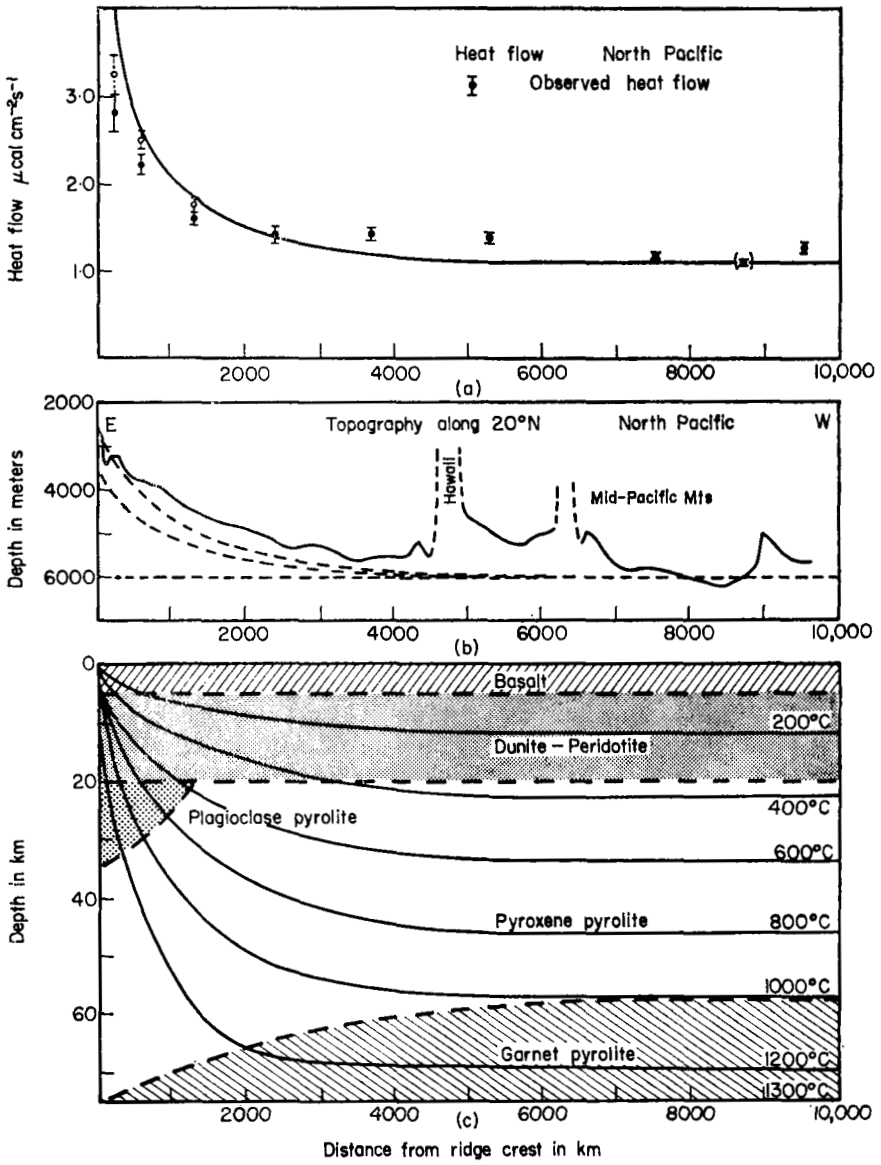

FIG. 17. (a) Comparison of observed heat flow averages in the North Pacific with the theoretical profile for a 75-km thick lithosphere. (b) Comparison of observed topography (solid line) (Udintsev 1964) with two theoretical profiles. The upper dashed curve is the profile expected from the thermal expansion and the phases of the model shown in (c). The lower dashed curve is the profile assuming thermal expansion of a lithosphere of uniform density. (c) Isotherms and chemical zoning of a 75-km thick lithosphere moving at 5 cm yr^{-1} to the right. The parameters are $T_1 = 1300$ °C, $K = 6{\cdot}15 \times 10^{-3}$ cal $°C^{-1}$ cm^{-1} s^{-1}, $H = 0{\cdot}1 \times 10^{-13}$ cal cm^{-3} s^{-1} $\Delta_c = 0{\cdot}3 \times 10^{-5}$ °C cm^{-1} (see Fig. 12 for explanation). The densities at 0 °C for plagioclase, pyroxene and garnet pyrolite are 3·26, 3·33 and 3·38 g cm^{-3} (Ringwood 1969). $\bar{\rho}_0$ (see Appendix I) is taken as 3·3 g cm^{-3}. The phase boundaries are for a ' wet ' pyrolite (Green 1969; Fig. 4).

In essence, the depleted model assumes an efficient convective process in the upper mantle which maintains a constant temperature at the bottom of the plate. The enriched model assumes a constant supply of heat from the deep mantle and requires an efficient differentiation process. These two contrasting models are essentially the same as those proposed by Bullard (1952) rephrased to fit modern ideas about the oceans. In spite of the difficulty in selecting a preferred geochemical model, the previous analysis has shown that the heat flow anomaly and topography of ridges can be accounted for satisfactorily by the creation of oceanic lithosphere. The thickness of the lithosphere is of the order of 100 km and the base of the lithosphere may have the temperature of incipient melting of pyrolite.

However, the basis for the previous analysis was an upper mantle with no phase changes. Though relevant experimental data on the subsolidus P–T stability fields is sparse, high pressure laboratory work in the past decade has shown that several phases are likely to be present in any model of the upper mantle. It is important to evaluate the effect of these phase changes on the surface elevation. To compute the increase in elevation resulting from the presence of several phases in a 75-km thick lithosphere, it is necessary, if we assume the bulk of the lithosphere to have the composition of pyrolite (Fig. 12), to consider a 'wet' upper mantle. In the presence of water, the pyrolite solidus is lowered and the temperature at the base of the lithosphere would be correspondingly decreased. The 'wet' pyrolite subsolidus stability fields of Green (1969; Fig. 4) were plotted on the temperature structure of a 75-km thick oceanic lithosphere with a basal temperature of 1300 °C. This temperature is the incipient melting of 'wet' pyrolite at that depth. As shown in Appendix I the effect on the surface elevation of density variations due to thermal expansion and phase changes can be added. Because of the lack of information on the thermal expansion of mantle materials, we have assumed the basalt, the ultrabasics and the pyrolite, all to have the same coefficient of thermal expansion. Rather arbitrarily, α was taken to be the coefficient of thermal expansion of pure olivine at high temperatures (Skinner 1966). The increase of elevation due to phase changes is of the order of 1 km at the crest of the ridge. Were the lithosphere 100 km thick, the additional elevation would be even greater and the theoretical profile would be considerably above the observed topography. Though the theoretical elevation for the 75-km thick lithosphere does not match the observed topography, a small variation in the high pressure and temperature fields for the plagioclase, pyroxene or garnet assemblages could easily yield a distribution of density contrast that would give a better fit. Further the stability fields at low temperatures and pressures are not well established. For example, it is possible that amphibole pyrolite be stable below the lid of ultrabasics. Considering these uncertainties, the difference between the theoretical and observed profiles (Fig. 17b) is not large enough to rule out a 75-km thick lithosphere. A slab of this thickness moving at 5 cm yr^{-1} gives a theoretical heat flow curve which lies close to the observed profile at distances greater than 2000 km from the ridge crest. A theoretical profile was not computed for the lower spreading rate near the axis. It can be seen from Fig. 15a that a decrease in spreading rate shifts the theoretical heat flow curve closer to the ridge axis. With a rate of 4 cm yr^{-1}, a fit to the heat flow near the crest could be obtained by assuming a bias in the observed values of no more than 30 per cent. Besides giving a better fit to the observed heat flow and topographic data, a 75-km thick lithosphere has a more realistic composition and is preferred from other lines of evidence such as surface wave dispersion studies (Kanamori & Abe 1968) and highly precise group velocity data (Press & Kanamori 1970).

This analysis was carried out for the composition of the enriched model where pyrolite is the major constituent of the lithosphere. MacGregor's (1968) P–T stability fields for plagioclase, spinel and garnet peridotite plotted on the temperature structure of a 75-km thick lithosphere would yield an increase in elevation comparable to that

produced by the pyrolite assemblages of Green (1969). Thus, phase changes are just as important in a depleted as in an enriched model.

The rate of heat loss from the Earth due to the production of lithosphere can be computed once the temperature structure in the slab is known (McKenzie & Sclater 1969). The derivation for the heat loss is given in Appendix I. If:

$$\rho = 3{\cdot}3 \text{ g cm}^{-3} \qquad C_p = 0{\cdot}25 \text{ cal g}^{-1} \text{ °C}^{-1}$$

$$L = 75 \times 10^5 \text{ cm} \qquad d = 5 \times 10^9 \text{ cm}$$

$$V = 3 \text{ cm yr}^{-1} \qquad \alpha = 4 \times 10^{-5} \text{ °C}^{-1}$$

$$H = 0{\cdot}10 \times 10^{-13} \text{ cal cm}^{-3} \text{ s}^{-1} \qquad T_1 - T_0 = 1300 \text{ °C}$$

$$K = 0{\cdot}066 \text{ cal °C}^{-1} \text{ cm}^{-1} \text{ s}^{-1} \qquad \Delta_c = 3{\cdot}0 \times 10^{-6} \text{ °C cm}^{-1}$$

then equation (23) of Appendix I yields a heat loss, for the production of lithosphere by all ridges, of

$$Q = 3{\cdot}6 \times 10^{12} \text{ cal s}^{-1}.$$

The total terrestrial heat loss is $7{\cdot}7 \times 10^{12}$ cal s^{-1} (Lee & Uyeda, 1965). The excess heat produced by creation of the lithosphere is approximately 45 per cent of the total average heat loss of the Earth. The only way this estimate can be reduced significantly is to decrease either the thickness of the lithosphere or the temperature at its base or both. At present there seem to be no strong arguments to reduce these parameters. It is likely that the creation of oceanic lithosphere has occurred during a significant portion of geologic history. The loss of heat by this process is large and may represent a major mode by which the Earth has cooled. It must be considered in any attempt to unravel the thermal history of the Earth.

11. Conclusions

The decrease of heat flow with age is well established for the continents (Polyak & Smirnov 1968; Smirnov 1968). The currently accepted hypothesis of plate tectonics predicts a similar decrease for the oceans but on a much shorter time scale (Langseth *et al.* 1966; McKenzie 1967). The heat flow observations in the North Pacific support this prediction. More heat flow measurements are needed in the other oceans to test whether the continuous decrease in heat flow with the age of the North Pacific floor is typical of all oceans. In these oceans more emphasis should be placed on measurements away from the crest of ridges and each region of different age should be given equal weight. The oldest provinces appear to be the most revealing in evaluating the flow of heat through the upper mantle. Measurements in the provinces close to the crest may be biased by the necessity of taking these measurements in sediment ponds. In the Pacific more detailed surveys should be made in these provinces to establish: (a) The effect of environment on the measurement of heat flow; and (b) the actual flow of heat through these provinces. If a reliable heat flow curve can be established for an ocean, it should be possible to tell the age of the ocean floor from the heat flow and also to test whether one model of the lithosphere can explain the heat flow decrease in all oceans. Thus, oceanic heat flow measurements may be a powerful tool in understanding the history of the oceans.

The two models which explain the near equality of heat flow through the continental shields and the old ocean basins within the framework of plate tectonics

require that the base of the oceanic plate be at a depth of between 75 and 100 km and that the continental plate be almost twice as thick. In both models, at depths of approximately 100 km, the temperatures are significantly higher under the oceans. This temperature distribution should be checked from induction studies. It would be of interest to compare transient variations in the magnetic field on the Australian shield with the same studies on the sea floor to the south.

The fit of the theoretical profiles to the observed heat flow and topography in the North Pacific depend critically on our knowledge of many crucial parameters. The computation of elevation is very sensitive to the choice of composition, the coefficient of thermal expansion, the basal temperature, and the P–T stability fields of subsolidus mineral assemblages. None of these are well known. The largest uncertainty of all is perhaps the chemical nature of the lower part of the lithosphere and the upper mantle. The presence of water has also been recognized as a very important factor for, as well as lowering the solidus temperature, it would also alter the stability fields of the phases present in the lithosphere. Considering these uncertainties, a 75-km thick oceanic lithosphere may well be found consistent with heat flow and topography of the North Pacific.

The difficulty in separating models with varying radioactive content arises through the uncertainty in the thermal conductivity K. However, there are several reasons for preferring the depleted model. A lithosphere with a low radioactivity will have a higher thermal conductivity. Recent work on a forsterite-rich olivine by Fukao (1969) has shown that, for the temperatures and pressures likely to exist in the lower part of the lithosphere, the thermal conductivity of ultrabasic rocks may be as high as $10{\cdot}0 \times 10^{-3}$ cal °C^{-1} cm^{-1} s^{-1}. The observed heat flow and elevation across the East Pacific Rise are better fit by theoretical models assuming a lithosphere with a thickness of 75 km if several phases are present. The surface wave dispersion data in the North Pacific also imply that the base of the lithosphere be at a depth close to 75 km. An enriched model of this thickness would have a heat production of $0{\cdot}45 \times 10^{-13}$ cal cm^{-3} s^{-1} for pyrolite II. Though not impossible such a high value seems unlikely. The depleted model is more appealing because it has a simpler differentiation history and its parameters lie comfortably within the allowed ranges rather than at the extreme ends.

Rocks dredged from the fracture zones that cut deeply through the oceanic crust (Engel & Fisher 1969) may yield information concerning the nature of the oceanic lithosphere. Careful dredging of these fracture zones followed by extensive chemical, petrological, trace element, and heat production studies are essential to set constraints on possible models of the oceanic lithosphere.

Acknowledgments

We would like to thank Professor V. Vacquier for bringing the Russian heat flow research to our knowledge. We are indebted to Dr D. P. McKenzie, Sir Edward Bullard and T. C. Hanks for pertinent reviews of the original manuscript. We also benefited from discussion with Drs J. Hawkins, R. L. Parker and H. W. Menard. Dr R. F. Roy kindly provided us with the data shown in Fig. 10. The figures were drawn by Linda Meinke. The calculations were effected on a heat flow model programme modified for the results presented here, originally written by Dr D. P. McKenzie of Cambridge University, England. This research was supported by the National Science Foundation and the Office of Naval Research.

University of California, San Diego,
Marine Physical Laboratory of the Scripps Institution of Oceanography,
La Jolla,
California 92037.

References

Anderson, E. M., 1939–1940. The loss of heat by conduction from the Earth's crust in Britain, *Proc. R. Soc.*, **60**, Part 2, Edinburgh.

Atwater, T. & Menard, H. W., 1970. Magnetic lineations in the north-east Pacific, *Earth Planet. Sci. Lett.*, **7**, 445–450.

Benfield, A. E., 1939. Terrestrial heat flow in Great Britian, *Proc. R. Soc. A.*, **173**, 428–450, London.

Birch, F., Roy, R. F. & Decker, E. R., 1968. Heat flow and thermal history in New England and New York, in *Studies of Appalachian Geology: Northern and. Maritime*, Chapter 33, ed. by W. White and E. an Zen, Interscience, New York

Blackwell, D. D., 1969. Heat flow determinations in the northwestern United States, *J. geophys. Res.*, **74**, 992–1007.

Brune, J. & Dorman, J., 1963. Seismic waves and Earth structure in the Canadian shield, *Bull. seism. Soc. Am.*, **53**, 167–210.

Bullard, E. C., 1939. Heat flow in South Africa, *Proc. R. Soc. A.*, **173**, 474–502, London.

Bullard, E. C., 1952. Discussion of paper by R. Revelle and A. E. Maxwell, Heat flow through the floor of the eastern north Pacific Ocean, *Nature, Lond.*, **170**, 200.

Bullard, E. C., 1968. Reversals of the Earth's magnetic field: The Bakerian Lecture, 1967, *Phil. Trans. R. Soc. A.*, **263**, 481–524, London.

Burns, R. E. & Grim, P. J., 1967. Heat flow in the Pacific Ocean off central California, *J. geophys. Res.*, **72**, 6239–6247.

Clark, S. P. & Ringwood, A. E., 1964. Density distribution and constitution of the mantle, *Rev. Geophys.*, **2**, 35–88.

Dickson, G. O., Pitman, W. C. & Heirtzler, J. R., 1968. Magnetic anomalies in the south Atlantic and ocean floor spreading, *J. geophys. Res.*, **73**, 2087–2100.

Engel, C. G. & Fisher, R. L., 1969. Lherzolite, anorthosite, gabbro and basalt dredged from the mid-Indian Ocean ridge, *Science*, **166**, 1136–1141.

Fisher, R. L., Von Herzen, R. P. & Rhea, K. P., 1967. Topographic heat flow studies in seven Micronesian and Melanesian trenches (abstract), *Trans. Am. geophys. Un.*, **48**, 218.

Fukao, Y., 1969. On the radiative heat transfer and the thermal conductivity in the upper mantle, *Bull. Earth. Res. Inst.*, **47**, 549–569.

Green, D. H., 1969. The origin of basaltic and nephelinitic magmas in the Earth's mantle, *Tectonophysics*, **7**, 409–422.

Green, D. H. & Ringwood, A. E., 1967. Genesis of basaltic magmas, *Bertr. Mineral. Petrol.*, **15**, 103–190.

Hamza, V. M. & Verma, R. K., 1969. The relationship of heat flow with age of basement rock, *Bull. Volcanologique*, **33**, 123–152.

Heirtzler, J. R., Dickson, G. O., Herron, E. M., Pitman, W. C. & Le Pichon, X., 1968. Marine magnetic anomalies, geomagnetic field reversals and motions of the ocean floor and continents, *J. geophys. Res.*, **73**, 2119–2136.

Holmes, A., 1965. *Principles of Physical Geology*, 1288 pp., Th. Nelson and Sons, Ltd., London and Edinburgh.

Hyndman, R. D., Lambert, I. B., Heier, K. S., Jaeger, J. C. & Ringwood, A. E., 1968. Heat flow and surface radioactivity measurements in the Precambrian shield of western Australia, *Phys. Earth Planet. Int.*, **1**, 129–135.

Kanamori, H. & Abe, K., 1968. Deep structure of island arcs as revealed by surface waves, *Bull. Earth .Res. Inst.*, **46**, 1001–1025.

King, P. B., 1969. Tectonic map of North America, Interior-Geological Survey Washington, D.C. G67154.

Kuno, H., 1967. Volcanological and petrological evidence regarding the nature of the upper mantle, in *The Earth's Mantle*, 89–110, ed. by T. F. Gaskell, Academic Press, London and New York.

Lachenbruch, A. H., 1968. Preliminary geothermal model of the Sierra Nevada, *J. geophys. Res.*, **73,** 6977–6989.

Langseth, M. G., Le Pichon, X. & Ewing, M., 1966. Crustal structure of mid-ocean ridges, 5, Heat flow through the Atlantic Ocean floor and convection currents, *J. geophys. Res.*, **71,** 5321–5355.

Langseth, M. G. & Von Herzen, R. P. Heat flow through the floor of the world oceans, in *The Sea*, Vol. 4 (in press).

Lee, W. H. K. & Uyeda, S., 1965. Review of heat flow data, in *Terrestrial Heat Flow*, American Geophysical Union Monograph 8, 87–190.

Massey, F. J., 1951. The Kolmogorov–Smirnov test for goodness of fit, *J. Am. Stat. Assoc.*, **46,** 68–78.

Maxwell, A. E., 1969. Recent deep sea drilling results from the south Atlantic (abstract), *Trans. Am. geophys. Un.*, **50,** 113.

McDonald, G. J. F., 1963. The deep structure of continents, *Rev. Geophys.*, **1,** 587–665.

MacGregor, I. D., 1968. Mafic and ultramafic inclusions as indicators of the depth of origin of basaltic magmas, *J. geophys. Res.*, **73,** 3737–3745.

McKenzie, D. P., 1967. Some remarks on heat flow and gravity anomalies, *J. geophys. Res.*, **72,** 6261–6271.

McKenzie, D. P. & Sclater, J. G., 1969. Heat flow in the eastern Pacific and sea floor spreading, *Bull. Volcanologique*, **33-1,** 101–118.

McManus, D. A. & Burns, R. E., 1969. Scientific report on deep-sea drilling project, Leg V, *Ocean Industry*, **4,** 40–42.

Oxburgh, E. R. & Turcotte, D. L., 1969. Increased estimate for heat flow at oceanic ridges, *Nature, Lond.*, **223,** 1354–1355.

Polyak, B. G. & Smirnov, Ya. B., 1966. Heat flow in the continents, *Dokl. Akad. Nauk SSSR*, **168,** 170–172.

Polyak, B. G. & Smirnov, Ya. B., 1968. Relationship between terrestrial heat flow and the tectonics of continents, *Geotectonics*, 205–213.

Press, F. & Kanamori, H., 1970. How thick is the lithosphere (abstract), *Trans. Am. geophys. Un.*, **51,** 363.

Ringwood, A. E., 1958. Constitution of the mantle, 3, *Geochim. Cosmochim. Acta.*, **15,** 195–212.

Ringwood, A. E., 1969. Composition and evolution of the upper mantle, in *The Earth's Crust and Upper Mantle*, American Geophysical Union Monograph 13, 1–17.

Roy, R. F., Blackwell, D. D. & Birch, F., 1968. Heat generation of plutonic rocks and continental heat flow provinces, *Earth Planet. Sci. Lett.*, **5,** 1–12.

Scientific Staff, Leg VI, 1969. Deep sea drilling project, Leg VI, *Geotimes*, **14,** 13–17.

Sclater, J. G. & Corry, C. E., 1967. Heat flow, Hawaiian area, *J. geophys. Res.*, **72,** 3711–3715.

Sclater, J. G., Vacquier, V., Greenhouse, J. P. & Dixon, F. S., 1968. Melanesian subcontinent: Presentation and discussion of recent heat flow measurements (abstract), *Trans. Am. geophys. Un.*, **49,** 217.

Sclater, J. G., Mudie, J. D. & Harrison, C. G. A., 1970. Detailed geophysical studies on the Hawaiian arch near 24° 25′ N, 157° 40′ W: A closely spaced suite of heat flow stations, *J. geophys. Res.*, **75,** 333–348.

Simmons, G. & Nur, A., 1968. Granites: Relation of properties *in situ* to laboratory measurements, *Science*, **162,** 789–791.

Skinner, B. J., 1966. Thermal expansion, in *Handbook of Physical Constants*, Geological Society of America Memorandum, **97,** 75.

Sleep, N. H., 1969. Sensitivity of heat flow and gravity to the mechanism of sea floor spreading, *J. geophys. Res.*, **74**, 542–549.

Smirnov, Ya. B., 1968. The relationship between the thermal field and the structure and development of the Earth's crust and upper mantle, *Geotectonics*, **5**, 343–352.

Talwani, M., Le Pichon, X. & Ewing, M., 1965. Crustal structure of the midocean ridges, 2, Computed model from gravity and seismic refraction data, *J. geophys. Res.*, **70**, 341–352.

Udintsev, G. B., 1964. *Bathymetry of the Pacific Ocean*, Institute of Oceanology, Academy of Sciences, Moscow.

Uyeda, S., Vacquier, V., Yasui, M., Sclater, J., Sato, T., Lawson, J., Watanabe, T., Dixon, F., Silver, E., Fukao, Y., Sudo, K., Nishikawa, M. & Tanaka, T., 1967. Paper 42. Results of geomagnetic survey during the cruise of R/V *Argo* in western Pacific 1966 and the compilation of magnetic charts of the same area, *Bull. Earthq. Res. Inst.*, **45**, 799–814.

Vacquier, V., Uyeda, S., Yasui, M., Sclater, J. G., Corry, C. & Watanabe, T., 1966. Paper 73. Studies of the thermal state of the Earth. The 19th Paper: Heat flow measurements in the northwestern Pacific, *Bull. Earthq. Res. Inst.*, **44**, 1519–1535.

Vacquier, V., Sclater, J. G. & Corry, C. E., 1967. Paper 22. Studies of the thermal state of the earth. The 21st Paper: Heat flow, eastern Pacific, *Bull. Earthq. Res. Inst.*, **45**, 375–393.

Vine, F. J., 1966. Spreading of the ocean floor: New evidence, *Science*, **154**, 1405–1415.

Wakita, H., Nagasawa, H., Uyeda, S. & Kuno, H., 1967. Uranium, thorium and potassium contents of possible mantle materials, *Geochem. J.*, **1**, 183.

Appendix I

Temperature and heat flow

The general equation for the temperature within a moving material is

$$\rho C_p \left[\frac{\partial T}{\partial t} + \mathbf{v}.\nabla T \right] = K\nabla^2 T + H \qquad (1)$$

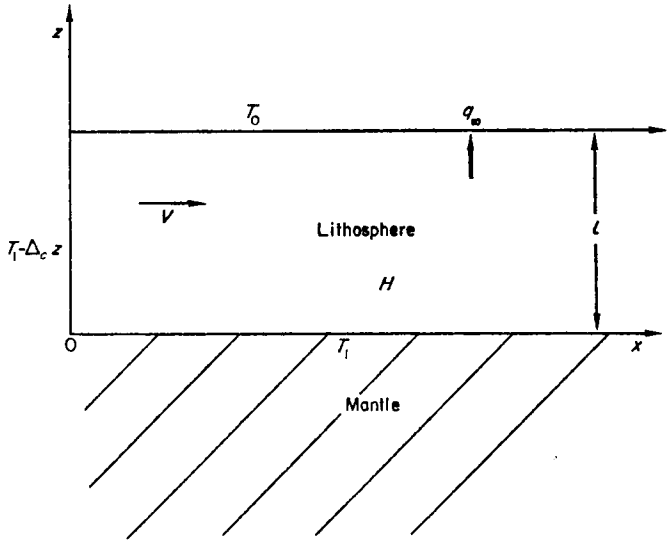

FIG. 18. Simple intrusive model (after McKenzie 1967).

where v is the velocity of the material, ρ its density, C_p its specific heat at constant pressure, K the thermal conductivity and H the rate of internal heat generation. For the case shown in Fig. 18 where v is directed along the x-axis equation (1) becomes:

$$\rho C_p v \frac{\partial T}{\partial x} = K\left(\frac{\partial^2 T}{\partial x^2} + \frac{\partial^2 T}{\partial z^2}\right) + H. \tag{2}$$

The time dependent term $\partial T/\partial t$ has been neglected for two reasons: It simplifies the solutions and, for the oceans considered, an approximately steady state has been reached. Following the notation of McKenzie (1967) we introduce the following non-dimensional variables:

$$\left.\begin{aligned} x &= lx' \\ z &= lz' \\ T &= (T_1 - T_0)\, T' + T_0 \\ H &= A_1\, A' \end{aligned}\right\} \tag{3}$$

substitution into (2) gives:

$$\frac{\partial^2 T'}{\partial x'^2} - 2R\frac{\partial T'}{\partial x'} + \frac{\partial^2 T'}{\partial z'^2} - B_1 A' = 0 \tag{4}$$

where R is the thermal Reynolds number.

$$R = \rho C_p \frac{vl}{2K}. \tag{5}$$

The boundary conditions for this problem are those of McKenzie (1967) except that at $x' = 0$:

$$\left.\begin{aligned} z' &= 0 \qquad T' = 1 \\ z' &= 1 \qquad T' = 0 \quad \text{for all } x' \\ x' &= 0 \qquad T' = 1 - \frac{\Delta_c l z'}{T_1 - T_0} = 1 - Dz' \end{aligned}\right\} \tag{6}$$

Δ_c, $0{\cdot}3\,^{\circ}\mathrm{C\,km^{-1}}$, is the adiabatic temperature gradient. The rate of internal heat generation, H, is assumed constant throughout the plate. The solution of equation (4) under these conditions is:

$$T' = 1 + \frac{B_1 A'}{2} z'^2 - \left(1 + \frac{B_1 A'}{2}\right) z' + \sum_{n=1}^{\infty} A_n \exp\{[R - \sqrt{(R^2 + n^2\pi^2)}]\, x'\} \sin n\pi z'$$

where

$$A_n = \frac{2(-1)^{n+1}}{n\pi}[1 - D] + \frac{2B_1 A'}{n^3 \pi^3}[1 - (-1)^n] \tag{7}$$

and

$$-\left(\frac{\partial T'}{\partial z'}\right)_{z'=1} = 1 - \frac{B_1 A'}{2} + 2\left\{\begin{aligned} &\sum_{n=1}^{\infty}\left(1 - D + \frac{2B_1 A'}{n^2\pi^2}\right)\exp\{[R - \sqrt{(R^2 + n^2\pi^2)}]\, x'\} \\ &n \text{ odd} \\ &\sum_{n=2}^{\infty}(1 - D)\exp\{[R - \sqrt{(R^2 + n^2\pi^2)}]\, x'\}. \\ &n \text{ even} \end{aligned}\right. \tag{8}$$

If we neglect all terms in the sum except $n = 1$ and remark that $R^2 \gg \pi^2$ we have:

$$-\left(\frac{\partial T'}{\partial z'}\right)_{z'=1} \simeq 1-\frac{B_1 A'}{2}+2\left(1-D+\frac{2B_1 A'}{\pi^2}\right)\exp\left(\frac{-\pi^2 x'}{2R}\right). \tag{9}$$

If q_∞ is the heat flow measured at the surface of the plate at great distance from the crest of the ridge (9) yields:

$$q_\infty \simeq \frac{K(T_1-T_0)}{l}+\frac{Hl}{2} \tag{10}$$

q_∞ is measured and H and l are assumed in the geochemical model chosen for the oceanic model. T_1 is the temperature of incipient melting of pyrolite at depth l. Under these conditions the thermal conductivity has to be equal to:

$$K = \frac{l}{T_1-T_0}\left(q_\infty-\frac{Hl}{2}\right). \tag{11}$$

If
$$T_0 = 0\,^\circ\mathrm{C}$$
$$l = 1{\cdot}0\times10^7\ \mathrm{cm}$$
$$H = 0{\cdot}1\times10^{-13}\ \mathrm{cal\,cm^{-3}\,s^{-1}}$$
$$q_\infty = 1{\cdot}1\times10^{-6}\ \mathrm{cal\,cm^{-2}\,s^{-1}}$$

then
$$T_1 = 1475\,^\circ\mathrm{C}$$

and
$$K = 7{\cdot}1\times10^{-3}\ \mathrm{cal\,^\circ C^{-1}\,cm^{-1}\,s^{-1}}.$$

If the half-width $\delta_{\frac{1}{2}}'$ of the heat flow anomaly is the value of x' such that:

$$-\left(\frac{\partial T'}{\partial z'}\right)_{z'=1} = 2$$

then:
$$\delta_{\frac{1}{2}}' = \frac{2R}{\pi^2}\log_e\left[\frac{4[5K(T_1-T_0-l\Delta_c)-Hl^2]}{5[2K(T_1-T_0)-Hl^2]}\right]. \tag{12}$$

But:
$$\delta_{\frac{1}{2}}' = \frac{\delta_{\frac{1}{2}}}{l} = \frac{vt_{\frac{1}{2}}}{l}$$

so that the heat flow should be
$$q_{\frac{1}{2}} = \frac{2K(T_1-T_0)}{l}$$

at a time
$$t_{\frac{1}{2}} = \frac{\rho C_p l^2}{K\pi^2}\log_e\left[\frac{4[5K(T_1-T_0-l\Delta_c)-Hl^2]}{5[2K(T_1-T_0)-Hl^2]}\right] \tag{13}$$

after the time of intrusion at the axis of the ridge of the corresponding material. This provides a means of checking directly if this radioactive model agrees with the curve of average heat flow within a province versus the age of the province.

Topography

If the elevation of the ridges above the surrounding ocean basins is due chiefly to thermal expansion of the lithosphere, this elevation can be computed (McKenzie & Sclater 1969). If isostatic compensation takes place at the bottom of the slab of

lithosphere at great distance from the crest of the ridge and if the mass of the lithosphere is conserved the shape of the slab must be as shown in Fig. 19. The mass of the two columns A and B can be equated:

$$\rho_w d_w + \int_0^l \rho_{sl_0} [1-\alpha T_\infty(z)]\,dz = \rho_w [d_w - le(x)] + \int_{le(x)}^{l[1+e(x)]} \rho_{sl_0} [1-\alpha T_x(z)]\,dz + \rho_{ast}\, l\varepsilon(x) \tag{14}$$

where ρ_w is the density of seawater, ρ_{sl_0} the density of the lithosphere at 0 °C, ρ_{ast} the density of the asthenosphere, α the thermal expansion coefficient, d_w the normal depth of an ocean basin far from a ridge crest, $le(x)$ the elevation of the ridge above the basin and $l\varepsilon(x)$ the elevation of the bottom of the lithosphere above the level of isostatic compensation.

Substitution of $T_\infty(z)$ and $T_x(z)$ from (7) into (14) and integration with respect to z yields:

$$e(x) = \frac{\alpha\rho_{sl_0}(T_1 - T_0)}{(\rho_{sl_0} - \rho_w) - \alpha\rho_{sl_0} T_0 + \alpha\rho_w T_1} \times \sum_{k=0}^{\infty} \left[\frac{4(1-D)}{(2k+1)^2\pi^2} + \frac{8B_1 A'}{(2k+1)^4\pi^4}\right] \exp\left\{\left[R - \sqrt{(R^2 + (2k+1)^2\pi^2)}\right]\frac{x}{l}\right\} \tag{15}$$

if terms in $e^2(x)$ are neglected and $\rho_{ast}\,\varepsilon(x) = \rho_w\, e(x)$ with $\rho_{ast} \simeq \rho_{sl_0}$. The elevation $le(0)$ at the crest of the ridge is:

$$le(0) \simeq \frac{\alpha l \rho_{sl_0}(T_1 - T_0)}{\rho_{sl_0} - \rho_w}\left[\tfrac{1}{2}(1-D) + \frac{8B_1 A'}{100}\right] \tag{16}$$

since

$$\sum_{k=0}^{\infty} \frac{1}{(2k+1)^2} \simeq 1{\cdot}23, \qquad \sum_{k=0}^{\infty} \frac{1}{(2k+1)^4} \simeq 1{\cdot}01$$

and

$$\rho_{sl_0} - \rho_w \gg \alpha\rho_{sl_0} T_0.$$

Substitution of:

$$\rho_{sl_0} = 3{\cdot}3\ \mathrm{g\,cm^{-3}}$$
$$\rho_w = 1\ \mathrm{g\,cm^{-3}}$$
$$\alpha = 4\times10^{-5}\ ^\circ\mathrm{C}^{-1}$$
$$T_1 = 1475\ ^\circ\mathrm{C}$$
$$T_0 = 0\ ^\circ\mathrm{C}$$
$$l = 1{\cdot}0\times10^{7}\ \mathrm{cm}$$
$$H = 0{\cdot}1\times10^{-13}\ \mathrm{cal\,cm^{-3}\,s^{-1}}$$
$$K = 7{\cdot}1\times10^{-3}\ \mathrm{cal\,^\circ C^{-1}\,cm^{-1}\,s^{-1}}$$
$$\Delta_c = 0{\cdot}3\times10^{-5}\ ^\circ\mathrm{C\,cm^{-1}}$$

gives:

$$B_1 A' = \frac{-Hl^2}{K(T_1 - T_0)} = -0{\cdot}095$$

$$D = \frac{l\Delta_c}{T_1 - T_0} = 0{\cdot}022$$

so that:

$$le(0) = 4{\cdot}0\times10^{5}\ \mathrm{cm} = 4000\ \mathrm{m}.$$

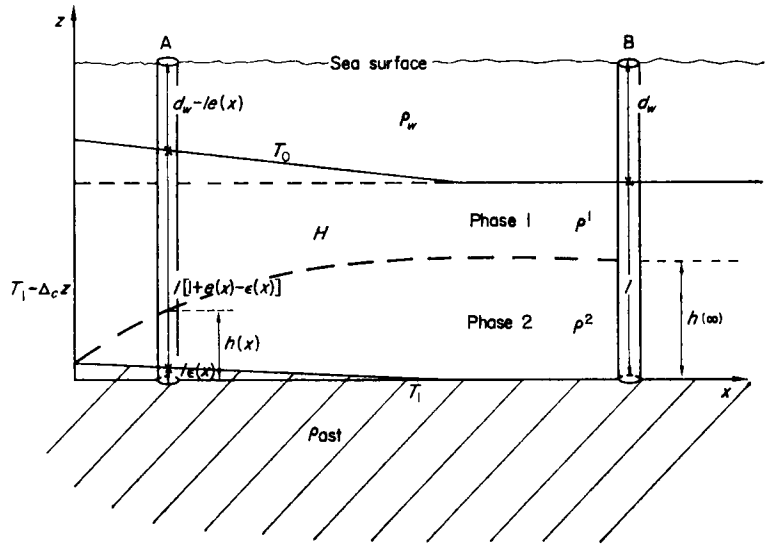

FIG. 19. Isostatic model of the oceanic lithosphere. A and B are two columns of unit area for the base and equal mass. When no phase changes are considered the density of the lithosphere is ρ_{sl_0}.

Topography with phase changes

If we assume a chemical composition for the lithosphere, the effect of phase changes on the topography can be computed. The subsolidus P–T stability fields are plotted on a cross section of the lithosphere. For simplicity we will consider the case where only two phases are stable in the lithosphere. The two phases are assumed to have the same coefficient of thermal expansion. Their densities are:

$$\left.\begin{aligned} \rho_0{}^1 &= \bar{\rho}_0 + \delta\rho_1 \\ \rho_0{}^2 &= \bar{\rho}_0 + \delta\rho_2 \end{aligned}\right\} \tag{17}$$

where $\delta\rho_1$ and $\delta\rho_2$ are small compared with $\bar{\rho}_0$, the mean density at 0 °C. Again assuming isostatic compensation takes place at the bottom of the lithosphere (Fig. 19) we can write:

$$\rho_w d_w + \int_0^l (\bar{\rho}_0 + \delta\rho)[1 - \alpha T_\infty(x)]\,dz = \rho_w [d_w - le_1(x)] + \rho_{ast} l\varepsilon_1(x) + \int_{l\varepsilon_1(x)}^{l[1+e_1(x)]} (\bar{\rho}_0 + \delta\rho)[1 - \alpha T_x(z)]\,dz. \tag{18}$$

Evaluating the integrals for intervals where the density $\bar{\rho}_0 + \delta\rho$ remains constant gives:

$$e_1(x) = \frac{\alpha\bar{\rho}_0(T_1 - T_0)}{\bar{\rho}_0 - \rho_w - \sigma\bar{\rho}_0\, T_0 + \delta\rho_1} \times \left\{ \sum_{k=0}^{\infty} \left[\frac{4(1-D)}{(2k+1)^2\,\pi^2} + \frac{8B_1\,A'}{(2k+1)^4\,\pi^4} \right] \exp\left\{ \left[R - \sqrt{(R^2 + (2k+1)^2\,\pi^2)} \right] \frac{x}{l} \right\} \right\} + \frac{(\delta\rho_2 - \delta\rho_1)(h(\infty) - h(x))}{(\bar{\rho}_0 - \rho_w - \alpha\bar{\rho}_0\, T_0 + \delta\rho_1)\, l} \tag{19}$$

if all terms in $\alpha\delta\rho$ are ignored. In this expression $h(x)$ is the height above the level of isostatic compensation at which the phase transformation takes place.

If we write $e_1(x) = e(x)+\delta e(x)$ equation (19) gives:

$$\delta e(x) = \frac{(\delta\rho_2-\delta\rho_1)}{(\bar{\rho}_0-\rho_w-\alpha\bar{\rho}_0\, T_0+\delta\rho_1)}\ \frac{(h(\infty)-h(x))}{l} \tag{20}$$

and $e(x)$ has the same form as the expression, equation (15), found for thermal expansion of a medium of density $\bar{\rho}_0$ at 0 °C since $\delta\rho_1$ is small in comparison with $\bar{\rho}_0-\rho_w$.

This indicates that the elevation $le_1(x)$ due to phase changes and thermal expansion of the lithosphere can be calculated by adding the elevation $l\delta e(x)$ due to phase changes alone for a uniform temperature to the elevation $le(x)$ due to thermal expansion alone for a medium of uniform density. This result is valid only to first order and requires that the phases vary little in density and have the same coefficient of thermal expansion.

Heat loss due to production of lithosphere

McKenzie & Sclater (1969) have shown that the rate of heat loss due to creation of lithosphere can be computed by considering the change in heat content of the lithosphere as it moves from the axis to the flanks of the ridge. When the lithosphere is produced it contains:

$$2\left\{\rho_{sl_0} C_p l\left[T_1(1-\alpha T_1)+\Delta_c\left(\alpha l T_1-\frac{l}{2}-\frac{\alpha\Delta_c l^2}{3}\right)\right]+Hl\right\}\ \text{cal unit area}^{-1} \tag{21}$$

At great distance from the ridge the heat content, neglecting terms in $\alpha B_1 A'$, is:

$$2\left\{\rho_{sl_0} C_p l\left[\frac{T_1+T_0}{2}-\frac{B_1 A'}{12}(T_1-T_0)-\frac{\alpha}{3}(T_1^2+T_0^2+T_1 T_0)\right]+Hl\right\}$$

$$\text{cal unit area}^{-1}. \tag{22}$$

The heat lost by plate creation for a total length of ridges of d cm and a mean spreading velocity of v cm yr^{-1} is:

$$2\rho_{sl_0} C_p l dv\left[\frac{T_1-T_0}{2}+\frac{B_1 A'}{12}(T_1-T_0)-\frac{\alpha}{3}(2T_1^2-T_0^2-T_1 T_0)\right.$$

$$\left.+\Delta_c\left(\alpha l T_1-\frac{l}{2}-\frac{\alpha\Delta_c l^2}{3}\right)\right]\ \text{cal s}^{-1}. \tag{23}$$